nature cell biology

Cdk5-mediated phosphorylation of endophilin B1 is required for induced autophagy in models of Parkinson's disease

Alan S. L. Wong[1,2,3], Rebecca H. K. Lee[1,2,3], Anthony Y. Cheung[1,2,3], Patrick K. Yeung[4], Sookja K. Chung[4,5], Zelda H. Cheung[1,2,3,6] and Nancy Y. Ip[1,2,3,6]

Cyclin-dependent kinase 5 (Cdk5) is a serine/threonine kinase that is increasingly implicated in various neurodegenerative diseases. Deregulated Cdk5 activity has been associated with neuronal death, but the underlying mechanisms are not well understood. Here we report an unexpected role for Cdk5 in the regulation of induced autophagy in neurons. We have identified endophilin B1 (EndoB1) as a Cdk5 substrate, and show that Cdk5-mediated phosphorylation of EndoB1 is required for autophagy induction in starved neurons. Furthermore, phosphorylation of EndoB1 facilitates EndoB1 dimerization and recruitment of UVRAG (UV radiation resistance-associated gene). More importantly, Cdk5-mediated phosphorylation of EndoB1 is essential for autophagy induction and neuronal loss in models of Parkinson's disease. Our findings not only establish Cdk5 as a critical regulator of autophagy induction, but also reveal a role for Cdk5 and EndoB1 in the pathophysiology of Parkinson's disease through modulating autophagy.

Cdk5 is a proline-directed serine/threonine kinase that is activated on binding to the neural-specific activators p35 and p39. Cdk5 modulates many cellular processes, including neuronal migration, survival, differentiation and synaptic functions[1–3]. Whereas basal Cdk5 activity is important for neuronal survival[4–6], aberrant Cdk5 activation is associated with neurodegenerative conditions. For example, calpain-mediated generation of p25 from p35 has been observed in neurodegenerative disorders such as Parkinson's disease, Alzheimer's disease and Huntington's disease[7–10]. As the most common movement disorder, Parkinson's disease is characterized by dopaminergic neuron loss in the substantia nigra and the presence of Lewy bodies composed predominantly of aggregated α-synuclein. Despite its prevalence, the pathogenic mechanism underlying Parkinson's disease remains enigmatic[11,12]. Interestingly, Cdk5 has been demonstrated to exhibit a critical role in 1-methyl-4-phenyl-1,2,3,6-tetrahydropyridine (MPTP)-mediated neuronal toxicity, one of the best characterized Parkinson's disease models[7,9,13]. MPTP, a neurotoxin that leads to selective degeneration of the substantia nigra neurons[12], increases Cdk5 activity and triggers neuronal loss through inactivation of survival factor MEF2 (myocyte enhancer factor 2), antioxidant enzyme Prx2 (peroxiredoxin 2) and DNA damage repair enzyme Ape1 (apurinic/apyrimidinic endonuclease 1; refs 9,13,14).

Autophagy (also known as macroautophagy) is a homeostatic process for the turnover of cytoplasmic contents and organelles through the engulfment of cargo into double-membraned autophagosomes, which subsequently fuse with endosomes and lysosomes for cargo degradation[15,16]. Recently, deregulation of autophagy has been linked with Parkinson's disease. Autophagosome accumulation is evident in Parkinson's disease brains[17,18] and in Parkinson's disease models including MPTP toxicity and overexpression of the α-synuclein^{A53T} mutant[19–22]. Although basal levels of autophagy and chaperone-mediated autophagy are critical for the clearance of α-synuclein aggregates[23–27], excessive autophagy has also been associated with neuronal loss[28,29]. Whether autophagy activation in Parkinson's disease is protective or detrimental therefore remains unknown. Here we report a further mechanism by which Cdk5 contributes to neuronal loss in Parkinson's disease models. We identify EndoB1, a protein previously implicated in autophagy induction in fibroblasts[30], as a Cdk5 substrate and show that its phosphorylation is required for autophagy induction and neuronal loss in Parkinson's disease models.

[1]Department of Biochemistry, The Hong Kong University of Science and Technology, Clear Water Bay, Kowloon, Hong Kong, China. [2]Molecular Neuroscience Center, The Hong Kong University of Science and Technology, Clear Water Bay, Kowloon, Hong Kong, China. [3]State Key Laboratory of Molecular Neuroscience, The Hong Kong University of Science and Technology, Clear Water Bay, Kowloon, Hong Kong, China. [4]Department of Anatomy, Li Ka Shing Faculty of Medicine, The University of Hong Kong, Hong Kong, China. [5]Research Centre of Heart, Brain, Hormone and Healthy Aging, Li Ka Shing Faculty of Medicine, The University of Hong Kong, Hong Kong, China.
[6]Correspondence should be addressed to Z.H.C. or N.Y.I. (e-mail: zelda@ust.hk or boip@ust.hk)

Received 2 September 2010; accepted 27 January 2011; published online 17 April 2011; DOI: 10.1038/ncb2217

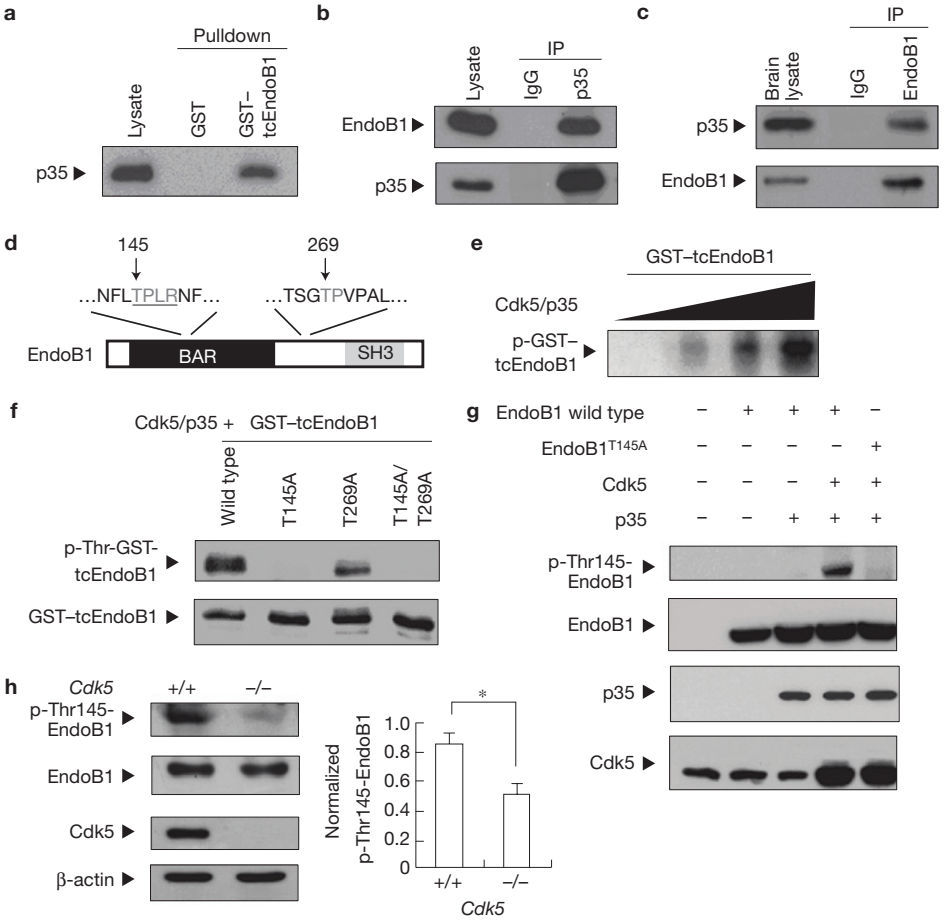

Figure 1 EndoB1 is a substrate of Cdk5/p35. (**a**) p35 interacts with EndoB1 in a GST pulldown assay. (**b**,**c**) EndoB1 co-immunoprecipitates (IP) with p35 in COS-7 cell lysates expressing p35 and full-length EndoB1 (**b**) and adult rat brain lysate (**c**). (**d**) Putative Cdk5 phosphorylation site(s) in the EndoB1 sequence. Two proline-directed threonine residues (arrows) are present with a Cdk5 consensus site found at Thr 145 (underlined). (**e**) Dose-dependent phosphorylation of EndoB1 by Cdk5/p35 in an *in vitro* kinase assay. (**f**) Cdk5/p35 phosphorylates EndoB1 at Thr 145 in an *in vitro* kinase assay. (**g**) Cdk5/p35 phosphorylates EndoB1 at Thr 145 in COS-7 cells. (**h**) Cdk5 phosphorylates EndoB1 at Thr 145 in *Cdk5*$^{+/+}$, but not *Cdk5*$^{-/-}$ mouse brains. Quantification of p-Thr145-EndoB1 level is shown in the right panel. Data are means ± s.e.m.; $n = 3$. Uncropped images of blots are shown in Supplementary Fig. S8.

RESULTS

Cdk5 phosphorylates EndoB1 at Thr 145

A yeast two-hybrid screen was carried out, in which a truncated form of EndoB1 (tcEndoB1) was identified as a p35-interacting protein (data not shown). EndoB1 is a lipid-binding protein that is concentrated on internal membranes[31–34]. We found that glutathione *S*-transferase (GST)–tcEndoB1, but not GST alone, pulled down p35 from COS-7 cell lysates overexpressing p35 (Fig. 1a). Furthermore, p35 co-immunoprecipitated with full-length EndoB1 in COS-7 cells overexpressing EndoB1 and p35 (Fig. 1b) and brain lysates (Fig. 1c), indicating that p35 associates with EndoB1 in the brain.

Sequence analysis revealed that EndoB1 contains two potential Cdk5 phosphorylation sites at Thr 145 and Thr 269 (Fig. 1d). GST–tcEndoB1, which contains both potential Cdk5 phosphorylation sites, was phosphorylated by Cdk5/p35 in a dose-dependent manner (Fig. 1e). To confirm the phosphorylation site(s), we mutated Thr 145 or Thr 269, or both, to alanine. Cdk5/p35 failed to phosphorylate GST–tcEndoB1^{T145A}, whereas mutation of Thr 269 only slightly reduced the level of EndoB1 phosphorylation (Fig. 1f), suggesting that Cdk5 predominantly phosphorylates EndoB1 at Thr 145. Overexpression of full-length wild-type EndoB1 or EndoB1^{T145A} together with Cdk5/p35 in COS-7 cells confirmed these observations. Whereas no Thr 145-phosphorylated EndoB1 was detected in the absence of Cdk5/p35 expression or when T145A EndoB1 was expressed, overexpression of Cdk5/p35 significantly increased Thr 145 phosphorylated EndoB1 (Fig. 1g), demonstrating that EndoB1 is phosphorylated at Thr 145 by Cdk5. Importantly, the level of Thr 145-phosphorylated EndoB1 was significantly reduced in the brains of *Cdk5*$^{-/-}$ mice (Fig. 1h), revealing the importance of Cdk5 as an endogenous kinase for EndoB1 *in vivo*.

EndoB1 phosphorylation by Cdk5 mediates starvation-induced autophagy

To explore the physiological significance of EndoB1 Thr 145 phosphorylation by neural-specific Cdk5, its effects on autophagy in neurons were investigated, as EndoB1 has been implicated in autophagy induction in fibroblasts[30]. Autophagosome formation induced by starvation was monitored by measuring the processing of microtubule-associated protein light chain 3 (LC3), a cytosolic protein that on autophagy induction is processed from LC3-I to LC3-II through lipid conjugation[16,35]. We also visualized

LC3-II recruitment to autophagosomes through overexpression of a red fluorescent protein (RFP)–LC3 construct, which during autophagosome formation changes from a diffuse to a punctate pattern. Starvation of cortical neurons significantly increased the percentage of cells exhibiting RFP–LC3 puncta (Fig. 2a). Furthermore, starvation induced a marked increase in LC3-II levels that was significantly attenuated by 3-methyladenine (3-MA), an autophagy inhibitor (Fig. 2a). These observations indicated that starvation induces autophagy in cortical neurons.

Interestingly, knockdown of EndoB1 expression using a pSUPER construct encoding a short interfering RNA (siRNA) sequence against *EndoB1* essentially abrogated the increase in LC3-II levels induced by starvation, in addition to markedly reducing the percentage of starved neurons with RFP–LC3 puncta (Fig. 2b). To examine whether the effect of EndoB1 knockdown on the formation of RFP–LC3 puncta involved enhanced autophagosome degradation, neurons expressing RFP–LC3 were treated with the lysosomal inhibitors E64d and pepstatin A. We found that, whereas treatment with lysosomal inhibitor increased the basal level of cells containing RFP–LC3 puncta in both the control and EndoB1-knockdown cells, the effect of EndoB1 knockdown on starvation-induced RFP–LC3 punctum formation was minimal (Fig. 2b). Collectively, these observations revealed that EndoB1 expression is crucial for autophagy induction in starved neurons.

We next investigated the involvement of Cdk5 in autophagy regulation by EndoB1. Both Cdk5 activity and Thr 145-phosphorylated EndoB1 levels were significantly elevated in starved neurons (Fig. 2c). Treatment with the Cdk5-selective inhibitor roscovitine (Ros) abrogated induction of Thr 145-phosphorylated EndoB1 in cortical neurons, indicating that Cdk5 is essential for EndoB1 phosphorylation at Thr 145 during starvation (Fig. 2d). Furthermore, Ros markedly reduced the starvation-induced increase in the LC3-II level and the percentage of cells exhibiting RFP–LC3 puncta (Fig. 2d). Knockdown of Cdk5 expression essentially abrogated the starvation-induced increase in Thr 145 EndoB1 phosphorylation, LC3-II levels and the percentage of starved neurons exhibiting RFP–LC3 puncta (Fig. 2e). Interestingly, knockdown of Cdk5 expression also upregulated the level of LC3-II in control cells (Fig. 2e). Nonetheless, as the increase was not recapitulated by quantification of RFP–LC3 puncta, the elevation in LC3-II level may not reflect changes in autophagosome formation[36]. More importantly, overexpression of the EndoB1^{T145A} mutant, but not wild-type or the phospho-mimetic mutant of EndoB1 (T145E), inhibited the starvation-induced increase in LC3-II levels and the percentage of cells exhibiting RFP–LC3 puncta in cortical neurons (Fig. 2f). Collectively, our findings demonstrate that Thr 145 phosphorylation of EndoB1 is required for starvation-induced autophagy in neurons.

EndoB1 phosphorylation does not affect its lipid binding

EndoB1 contains an amino-terminal amphipathic helix and a BAR (Bin–Amphiphysin–Rvs) domain (N-BAR domain), and at the carboxy terminus an SH3 (SRC homology 3) domain[37]. The N-BAR domain mediates direct lipid binding for curving and tubulation of lipid bilayers[32], and is required for dimerization of endophilins, a step essential for promoting membrane curvature and recruitment of interacting proteins[34]. The SH3 domain is involved in the recruitment of cytoplasmic interacting partners. EndoB1 was shown to induce autophagy induction through direct association with UVRAG (ref. 30), a protein essential for autophagosome formation and maturation[38,39], through its SH3 domain. EndoB1 association with UVRAG recruits Beclin 1 to initiate autophagosome formation[30]. Interestingly, the N-BAR domain of EndoB1 is also required for autophagosome formation in fibroblasts[30–34]. We tested whether phosphorylation alters the lipid-binding property of EndoB1 to induce autophagy. To disrupt lipid binding, we generated a mutant of EndoB1 in which the five lysine/arginine residues between amino acids 176 and 183 were mutated to glutamic acid (5E). Lipid binding of the 5E mutant was markedly reduced, compared with wild-type EndoB1, when incubated in brain lipid extracts (Fig. 3a). In addition, dimerization of EndoB1 (Fig. 3b) and UVRAG recruitment (Fig. 3c) were abolished in the 5E mutant, indicating that the lipid-binding property of EndoB1 is critical for EndoB1 dimerization and UVRAG recruitment. Importantly, overexpression of the 5E EndoB1 mutant in neurons markedly reduced starvation-induced autophagy (Fig. 3d), revealing that lipid binding is required for the role of EndoB1 in autophagy induction in starved neurons.

Given that the Cdk5 phosphorylation site, Thr 145, is in the N-BAR domain, we tested whether phosphorylation affects EndoB1 binding to lipids. Interestingly, both purified full-length T145A and T145E mutants bound lipid at a comparable level, which was slightly reduced when compared with wild-type EndoB1, but the difference was not statistically significant (Fig. 3e). Similar observations were obtained using the purified N-BAR domain of wild-type, T145A and T145E EndoB1 (Supplementary Fig. S1), indicating that Thr 145 phosphorylation negligibly affected EndoB1 lipid binding. In addition, we tested whether Thr 145 phosphorylation regulates EndoB1 recruitment to Atg5 (autophagy-related 5)-positive vesicles. Consistent with earlier observation in fibroblasts[30], starvation triggered a marked increase in the co-localization of GFP-tagged wild-type EndoB1 signals with Atg5 immunoreactivity. Interestingly, GFP-tagged wild-type and EndoB1^{T145A} were recruited to Atg5-positive entities at comparable levels after starvation (Fig. 3f). Taken together, our observations indicate that Thr 145 phosphorylation of EndoB1 by Cdk5 does not substantially affect lipid binding of EndoB1 or its recruitment to Atg5-positive autophagic vacuoles.

EndoB1 phosphorylation enhances UVRAG binding

We next investigated whether Thr 145 phosphorylation regulates EndoB1 dimerization to modulate UVRAG recruitment. Interestingly, Cdk5/p35 overexpression significantly enhanced the dimerization of haemagglutinin (HA)-tagged EndoB1 with GFP-tagged EndoB1 (Fig. 4a). Furthermore, dimerization of EndoB1^{T145E} was markedly enhanced when compared with that of wild-type EndoB1 or EndoB1^{T145A} in the absence of Cdk5/p35 co-expression (Fig. 4b). We next investigated whether Cdk5 modulated UVRAG recruitment to EndoB1. Interestingly, EndoB1 and UVRAG co-immunoprecipitation was significantly reduced in *Cdk5*$^{-/-}$ brain lysates (Fig. 4c). Furthermore, the association of EndoB1^{T145A} with UVRAG (Fig. 4d) and Beclin 1 (Fig. 4e) was significantly weaker than that observed for wild-type EndoB1. We next carried out a gel-filtration assay using mouse brain extracts to examine the distribution of Thr 145-phosphorylated EndoB1 in relation to other proteins involved in autophagosome formation.

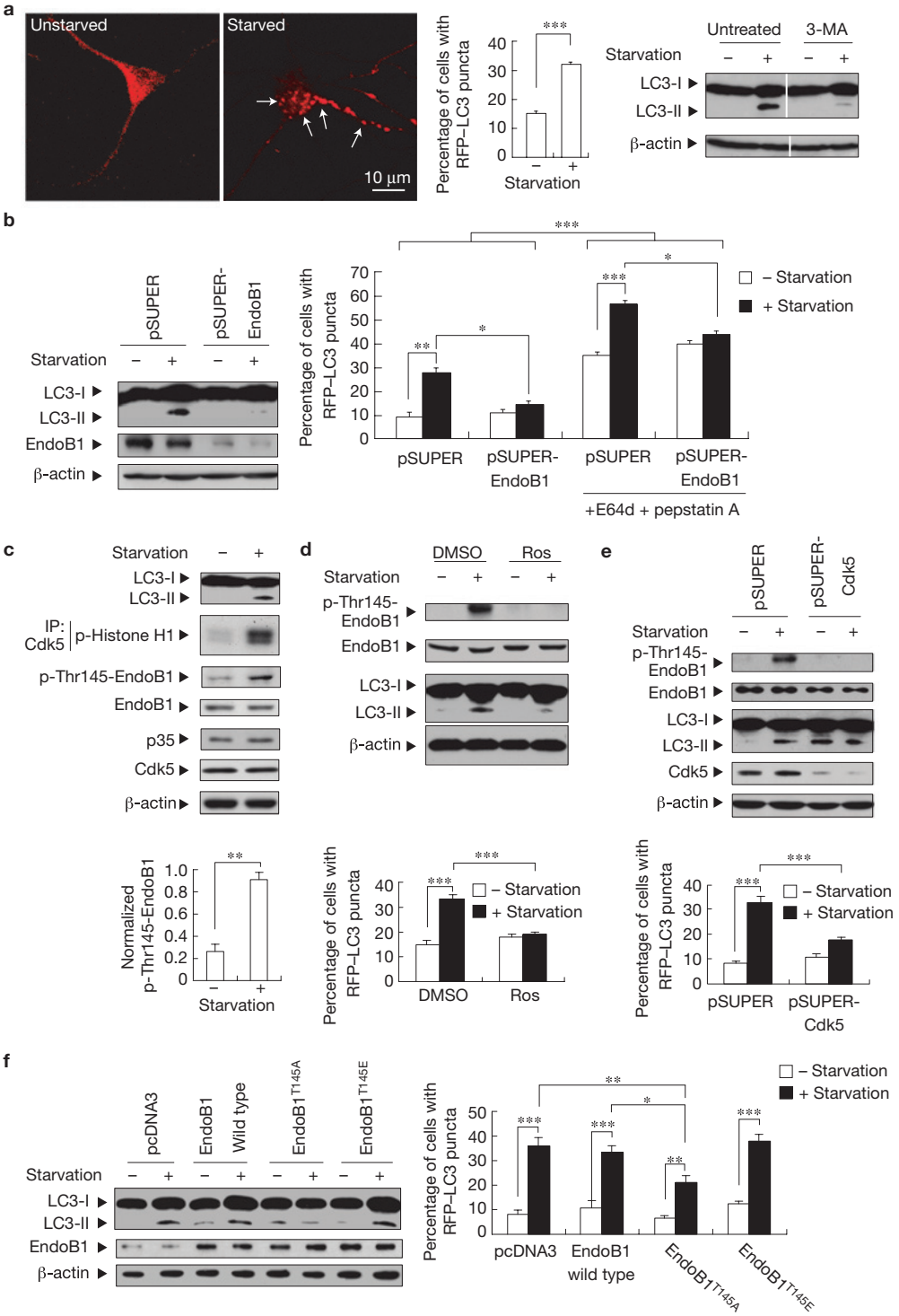

Figure 2 Cdk5-mediated phosphorylation of EndoB1 is required for starvation-induced autophagy in neurons. (**a**) Left: starvation increases the level of RFP–LC3 puncta (arrows) in rat cortical neurons. Middle: quantification of the percentage of cells with RFP–LC3 puncta. Right: pretreatment with 10 mM 3-MA attenuates the starvation-induced increase in LC3-II level in neurons. Data are means ± s.e.m.; $n = 3$. Samples were run on the same gel and spliced together to create the image shown. (**b**) Knockdown of EndoB1 abolishes the starvation-induced increase in LC3-II levels (left) and the percentage of cells with RFP–LC3 puncta (right) in neurons. Data are means ± s.e.m.; $n = 3$. (**c**) Starvation enhances Cdk5 activity (top) and increases the level of Thr 145-phosphorylated EndoB1 in neurons (top and bottom). Histone H1 was used as a Cdk5 substrate. Data are means ± s.e.m.; $n = 3$. (**d**,**e**) Pretreatment with Ros (**d**) or knockdown of Cdk5 (**e**) attenuates starvation-induced EndoB1 phosphorylation at Thr 145 and autophagy induction in neurons. Data are means ± s.e.m.; $n = 3$ for **d** and $n = 8$ for **e**. DMSO, dimethylsulphoxide. (**f**) Overexpression of EndoB1^{T145A} significantly reduces the starvation-induced increase in LC3-II levels (left) and the percentage of cells with RFP–LC3 puncta (right) in neurons. Data are means ± s.e.m.; $n = 6$. Uncropped images of blots are shown in Supplementary Fig. S8.

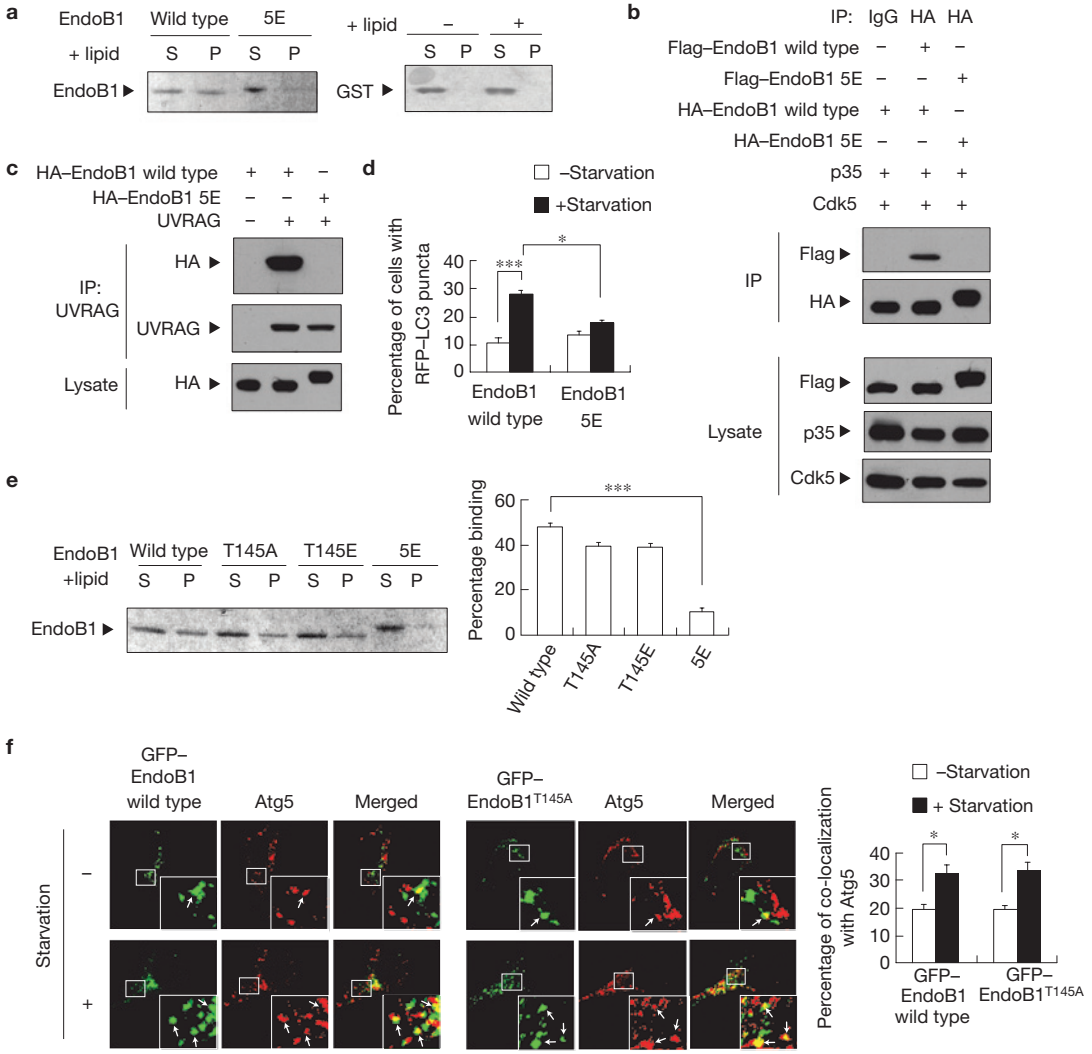

Figure 3 Thr 145 phosphorylation of EndoB1 does not affect its lipid binding and co-localization with Atg5. (**a**) Left: lipid binding of EndoB1 is inhibited by mutating the five lysine/arginine residues between amino acids 176 and 183 of EndoB1 to glutamic acid (5E mutant). Right: purified GST protein was included as a negative control. S, supernatant fraction; P, pellet fraction that contains the lipid-bound proteins. (**b**,**c**) The 5E mutant of EndoB1 fails to dimerize (**b**) and interact with UVRAG (**c**) in 293T cells. (**d**) Overexpression of the 5E mutant of EndoB1 blocks starvation-induced autophagy in cortical neurons. Data are means ± s.e.m.; $n = 3$. (**e**) Mutation of Thr 145 to alanine (T145A) or glutamic acid (T145E) has negligible effect on the lipid-binding property of EndoB1. Conversely, the 5E mutant is less able to bind lipid. The right panel shows quantified data as means ± s.e.m.; $n = 3$. (**f**) Starvation increases co-localization of GFP–EndoB1 (green) with Atg5 (red) in neurons. The T145A mutation of GFP–EndoB1 does not affect its co-localization with Atg5-positive entities. Arrows denote GFP–EndoB1- and Atg5- positive vesicles. The right panel shows quantified data as means ± s.e.m.; $n = 9$. Uncropped images of blots are shown in Supplementary Fig. S8.

Thr 145-phosphorylated EndoB1 was detected in fractions 24–26 of the membrane fraction of mouse brain lysates, co-eluting with UVRAG, Beclin 1, p35 and Cdk5 (Fig. 4f). In addition, we observed reduced EndoB1 levels in the membrane fractions of *Cdk5*$^{-/-}$ brain lysates, accompanied by increased EndoB1 levels in the cytoplasmic fractions (Supplementary Fig. S2). More importantly, co-immunoprecipitation of EndoB1 with Beclin 1 and UVRAG in wild-type mice was observed only in the fractions where Thr 145-phosphorylated EndoB1 was detected (Fig. 4g). In addition, co-immunoprecipitation of the three proteins was detected at fraction 26, which corresponded to the approximate molecular weight of a potential complex consisting of an EndoB1 dimer, UVRAG and Beclin 1 (Fig. 4g). These observations are consistent with earlier findings demonstrating that membrane-bound endophilins are dimers[34]. Our findings collectively suggest that Thr 145 phosphorylation of EndoB1 by Cdk5 favours EndoB1 dimerization, which then facilitates recruitment of UVRAG and Beclin 1 to trigger autophagosome formation.

EndoB1 phosphorylation by Cdk5 mediates autophagy in Parkinson's disease models

Deregulation of autophagy is increasingly implicated in the pathophysiology of Parkinson's disease. Given the emerging link between Cdk5 and neuronal loss triggered by MPTP toxicity, it is plausible that the effect of Cdk5 on EndoB1 and autophagy contributes to the pathophysiology of Parkinson's disease. We thus examined whether autophagy is induced in MPTP-injected mice. Consistent with earlier findings, injection of MPTP resulted in progressive degeneration of tyrosine hydroxylase-positive cells

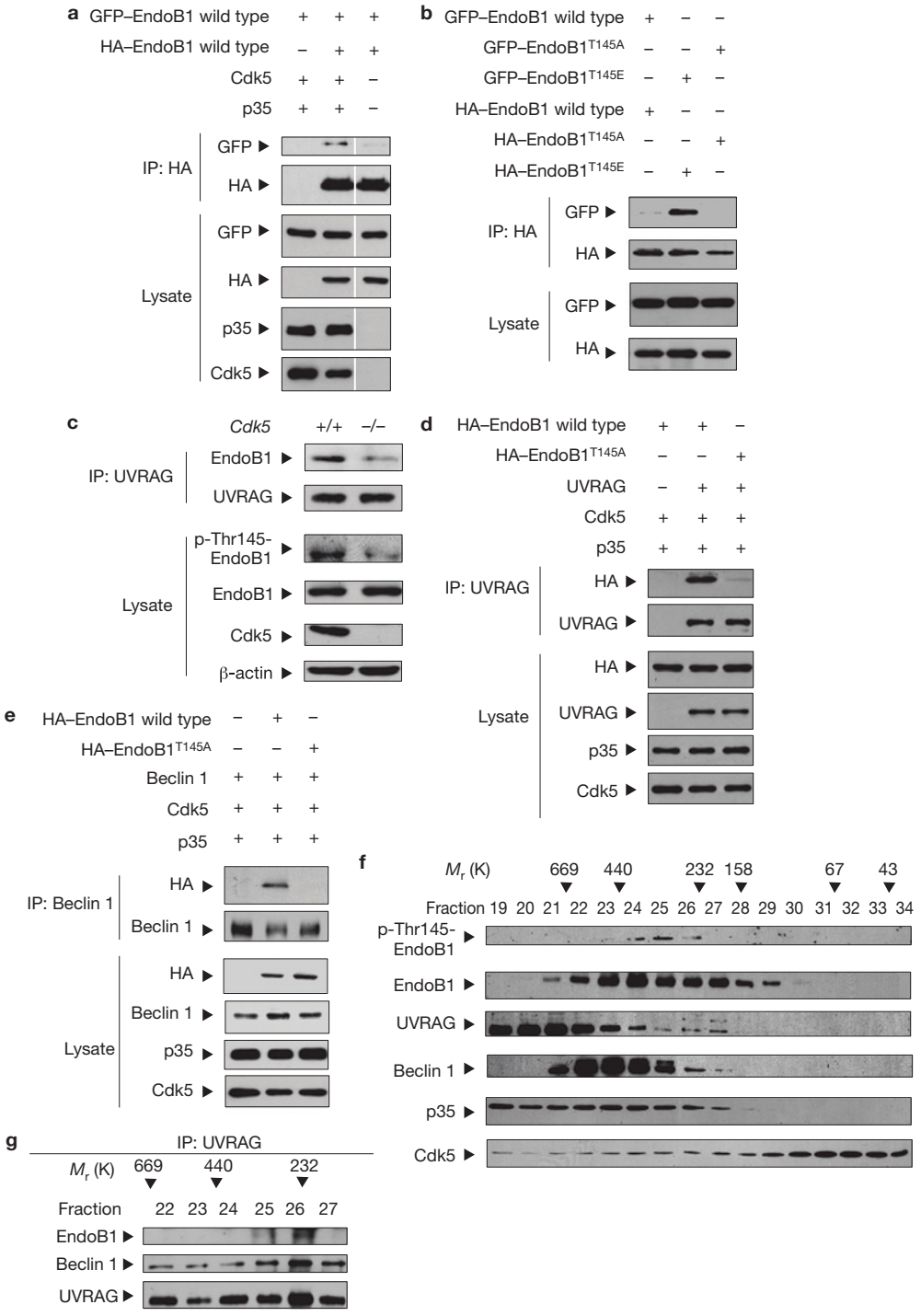

Figure 4 Cdk5-mediated Thr 145 phosphorylation of EndoB1 regulates its dimerization and interaction with UVRAG/Beclin 1. (**a**) Overexpression of Cdk5/p35 enhances EndoB1 dimerization in 293T cells. Samples were run on the same gel and spliced together to create the image shown. (**b**) Thr 145 phosphorylation of EndoB1 facilitates its dimerization in 293T cells. (**c**) Diminished interaction between EndoB1 and UVRAG in *Cdk5*$^{-/-}$ mouse brain lysates. (**d**,**e**) Thr 145 phosphorylation of EndoB1 enhances its interaction with UVRAG (**d**) and Beclin 1 (**e**) in 293T cells. (**f**,**g**) Gel-filtration analysis on the membrane fraction of mouse brain lysates. Fractions obtained were subjected to immunoblot analysis (**f**), or immunoprecipitation followed by immunoblotting (**g**). Uncropped images of blots are shown in Supplementary Fig. S8.

in the substantia nigra[7] (Fig. 5a). Interestingly, MPTP injection increased Thr 145-phosphorylated EndoB1 and LC3-II levels in the midbrain (Fig. 5b), whereas levels of EndoB1, Cdk5, p35 (Fig. 5b) and p25 (data not shown) remained unchanged. Furthermore, treatment with MPP^+ (1-methyl-4-phenylpyridinium) enhanced the LC3-II level (Supplementary Fig. S3a) and the percentage of cells with RFP–LC3 puncta (Fig. 5c) in cultured neurons. This was accompanied by an increase in Cdk5 activity, and an elevation in Thr 145-phosphorylated EndoB1 (Supplementary Fig. S3a). Knockdown of EndoB1 or Cdk5 expression both markedly attenuated

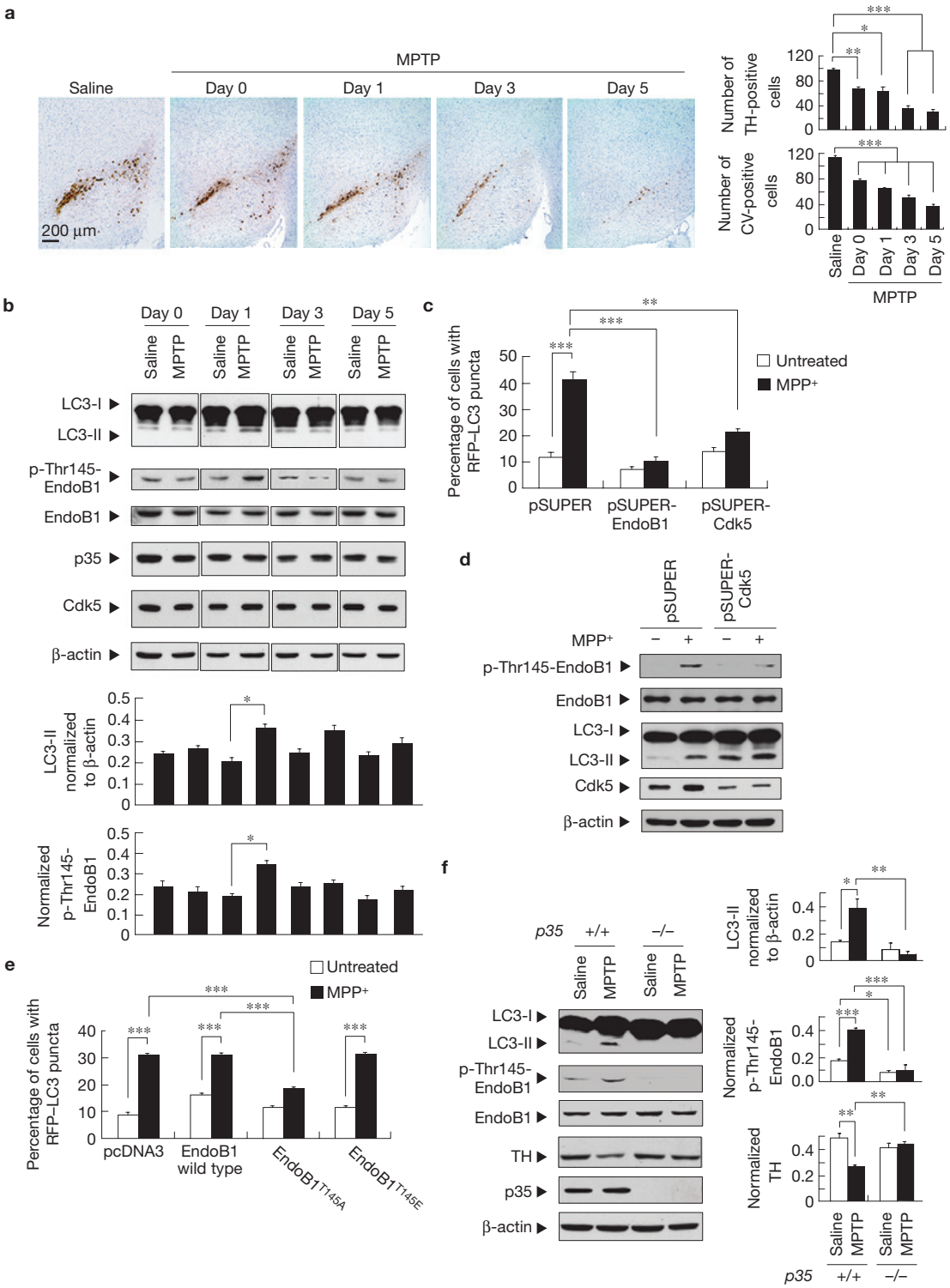

Figure 5 Cdk5-mediated Thr 145 phosphorylation of EndoB1 is involved in autophagy triggered by MPTP. (**a**) MPTP administration decreases the numbers of tyrosine hydroxylase (TH)- and cresyl violet (CV)-positive neurons in the substantia nigra. Representative images of tyrosine hydroxylase-stained brain sections are shown. Right panels show quantified data as means ± s.e.m.; $n = 9$ for tyrosine hydroxylase and $n = 3$ for cresyl violet. (**b**) MPTP administration upregulates the levels of LC3-II and Thr 145-phosphorylated EndoB1 in the midbrain. Lower panels show quantified data as means ± s.e.m.; $n = 3$. (**c**) Knockdown of EndoB1 or Cdk5 inhibits MPP^+-induced autophagy in cultured neurons. Data are means ± s.e.m.; $n = 5$. (**d**) Cdk5 mediates the MPP^+-induced EndoB1 phosphorylation at Thr 145 and the MPP^+-induced increase in the LC3-II level in neurons. (**e**) Overexpression of $EndoB1^{T145A}$ attenuates MPP^+-induced autophagy in neurons. Data are means ± s.e.m.; $n = 7$. (**f**) MPTP fails to increase LC3-II and Thr 145-phosphorylated EndoB1 levels in the midbrain of $p35^{-/-}$ mice. The concomitant reduction in tyrosine hydroxylase level triggered by MPTP injection is also markedly attenuated. Right panels show quantified data as means ± s.e.m.; $n = 3$. Uncropped images of blots are shown in Supplementary Fig. S8.

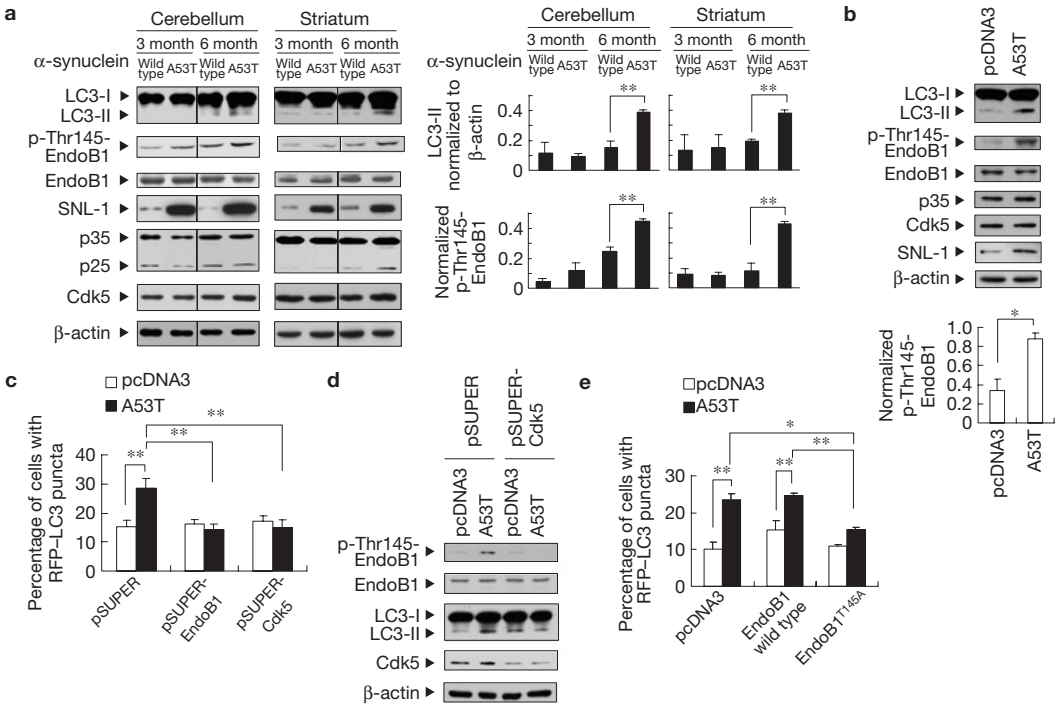

Figure 6 Thr 145 phosphorylation of EndoB1 by Cdk5 contributes to α-synuclein^{A53T} mutant-induced autophagy. (**a**) Upregulation of the levels of LC3-II and Thr 145-phosphorylated EndoB1 in the cerebellum and striatum of α-synuclein^{A53T} transgenic mice. Right panels show quantified data as means ± s.e.m.; $n = 3$. (**b**) Overexpression of α-synuclein^{A53T} mutant upregulates LC3-II level and Thr 145-phosphorylated EndoB1 in cultured neurons. Lower panel shows quantified data as means ± s.e.m.; $n = 3$. (**c**) Knockdown of EndoB1 or Cdk5 inhibits α-synuclein^{A53T} mutant-induced autophagy induction in neurons. Data are means ± s.e.m.; $n = 7$. (**d**) Cdk5 mediates α-synuclein^{A53T} mutant-induced Thr 145 phosphorylation of EndoB1 and the increase of LC3-II in neurons. (**e**) Overexpression of EndoB1^{T145A} attenuates α-synuclein^{A53T} mutant-induced autophagy in neurons. Data are means ± s.e.m.; $n = 7$. Uncropped images of blots are shown in Supplementary Fig. S8.

the MPP$^+$-induced increase in the percentage of cells exhibiting RFP–LC3 puncta (Fig. 5c). Knockdown of Cdk5 expression not only inhibited the induction of Thr 145 phosphorylation by MPP$^+$, but also abrogated the MPP$^+$-induced increase in LC3-II levels (Fig. 5d). In addition, overexpression of EndoB1^{T145A}, but not wild-type EndoB1 or EndoB1^{T145E}, significantly reduced the percentage of cells exhibiting RFP–LC3 puncta following MPP$^+$ treatment (Fig. 5e). These observations revealed that MPP$^+$ induces autophagy in neurons, and that Cdk5-mediated phosphorylation of EndoB1 at Thr 145 is essential for this induction. Furthermore, MPTP injection failed to increase LC3-II levels in the midbrain of p35-deficient mice (Fig. 5f). Concomitantly, MPTP-induced reduction in tyrosine hydroxylase levels was also abolished in p35-deficient mice (Fig. 5f). These observations provide further evidence that Cdk5 activity is essential for autophagy induction in the MPTP-toxicity model of Parkinson's disease.

We attempted to verify our findings with a second Parkinson's disease model, using mice expressing the α-synuclein^{A53T} mutant. A53T and A30P mutations of α-synuclein have been associated with familial Parkinson's disease[11]. Transgenic mice overexpressing the A53T mutant of α-synuclein recapitulate symptoms of Parkinson's disease patients, with the development of cytoplasmic inclusions, tremor, muscle rigidity and impairment of motor functions[40,41]. Interestingly, an increase in LC3-II levels was consistently observed in the cerebellum and striatum of 6-month-old animals. This was accompanied by elevation in Thr 145-phosphorylated EndoB1 (Fig. 6a) and enhanced recruitment of UVRAG to EndoB1 (data not shown). Furthermore, a slight increase in p25 was observed in the striatum (Fig. 6a). In agreement with our *in vivo* observations, overexpression of the α-synuclein^{A53T} mutant increased Thr 145-phosphorylated EndoB1, LC3-II levels (Fig. 6b) and the percentage of cells exhibiting RFP–LC3 puncta (Fig. 6c) in cultured neurons. Importantly, knockdown of Cdk5 in cells expressing the α-synuclein^{A53T} mutant not only abrogated the increase in Thr 145-phosphorylated EndoB1, but also reversed the elevation in LC3-II levels (Fig. 6d) and the percentage of cells with RFP–LC3 puncta (Fig. 6c). Furthermore, knockdown of EndoB1 (Fig. 6c) or overexpression of EndoB1^{T145A} (Fig. 6e) similarly abrogated the α-synuclein^{A53T} mutant-induced increase in the percentage of cells exhibiting RFP–LC3 puncta. Our observations demonstrate that Cdk5-mediated Thr 145 phosphorylation of EndoB1 is required for autophagy induction in cells expressing the α-synuclein^{A53T} mutant.

Neuronal loss in Parkinson's disease models requires EndoB1 phosphorylation by Cdk5

Previous studies have established autophagy as a protective mechanism critical for neuronal survival[42]. Knockdown of Atg5 or Atg7, proteins essential for autophagosome formation, leads to neurodegeneration[25,26]. Autophagy induction reduces huntingtin accumulation and neuronal loss in a model of Huntington's disease[27]. Nonetheless, excessive autophagy has also been associated with neuronal death[28]. Indeed, we found that starvation also led to significant neuronal loss in cortical neurons (Supplementary Fig. S4a). Knockdown of Atg5 expression, which inhibited the starvation-triggered increase in LC3-II levels (Supplementary Fig. S4b), also reduced neuronal survival in the

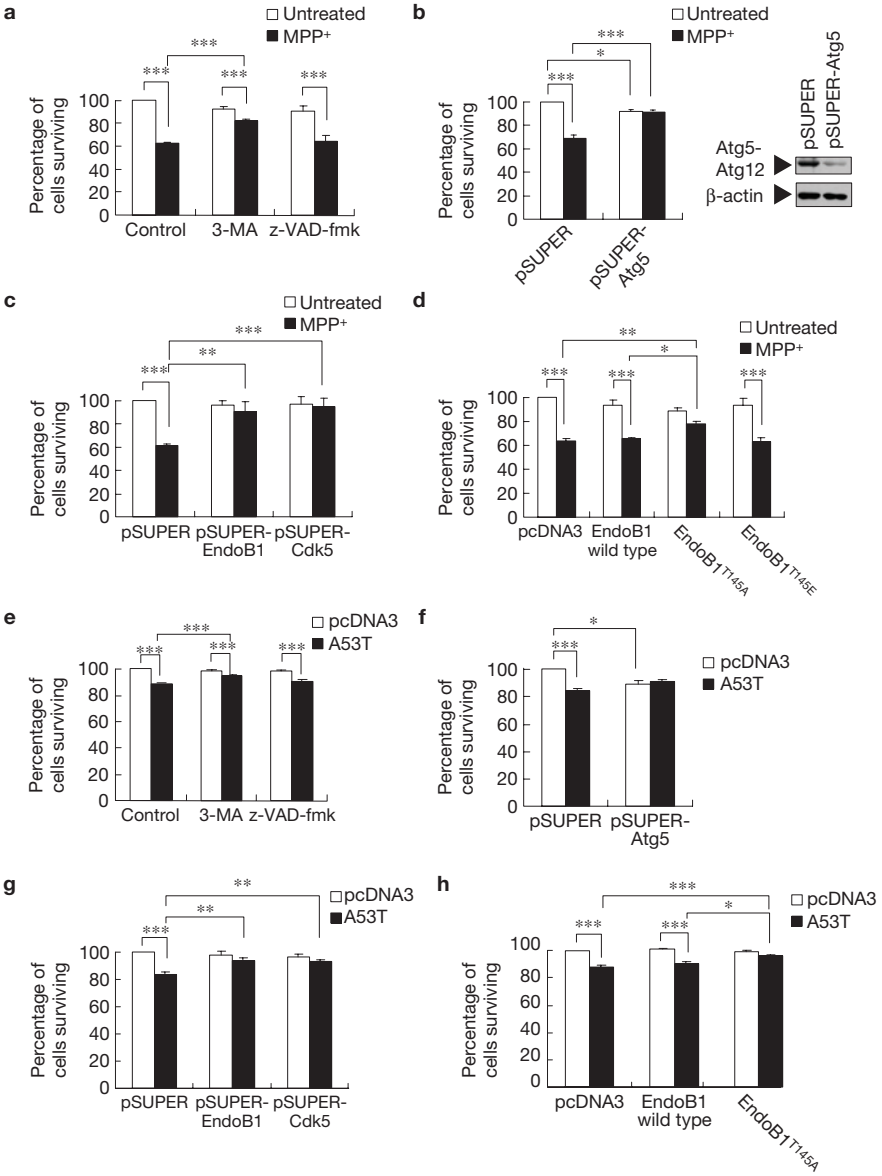

Figure 7 Cdk5-mediated Thr 145 phosphorylation of EndoB1 is required for MPP$^+$- and α-synuclein^{A53T} mutant-induced neuronal death. (**a**) Pretreatment with 3-MA, but not z-VAD-fmk, significantly reduces MPP$^+$-induced neuronal death. Data are means ± s.e.m.; $n = 6$. (**b**) Knockdown of Atg5 expression abrogates MPP$^+$-induced neuronal loss, whereas it reduces neuronal survival in untreated cells. Data are means ± s.e.m.; $n = 3$. (**c**) Knockdown of EndoB1 or Cdk5 expression abolishes MPP$^+$-induced neuronal death. Data are means ± s.e.m.; $n = 8$. (**d**) Overexpression of EndoB1^{T145A} inhibits MPP$^+$-induced neuronal death. Data are means ± s.e.m.; $n = 5$. (**e**) Pretreatment with 3-MA, but not z-VAD-fmk, reduces α-synuclein^{A53T} mutant-induced neuronal death. Data are means ± s.e.m.; $n = 6$. (**f**) Knockdown of Atg5 expression abolishes α-synuclein^{A53T} mutant-induced neuronal death, whereas it reduces neuronal survival in vector-transfected cells. Data are means ± s.e.m.; $n = 3$. (**g**) Knockdown of EndoB1 or Cdk5 expression abolishes α-synuclein^{A53T} mutant-induced neuronal death. Data are means ± s.e.m.; $n = 4$. (**h**) Expression of EndoB1^{T145A} inhibits α-synuclein^{A53T} mutant-induced neuronal death. Data are means ± s.e.m.; $n = 6$.

untreated cells, albeit to a lesser extent, confirming that the basal level of autophagy contributed to neuronal survival (Supplementary Fig. S4c). Nonetheless, Atg5 knockdown markedly attenuated starvation-induced neuronal loss (Supplementary Fig. S4c). In addition, Atg12 knockdown attenuated autophagy activation and reduced neuronal survival in untreated cells, whereas it reversed starvation-induced neuronal loss (Supplementary Fig. S5a,b). We also examined the effect of the mTOR (mammalian target of rapamycin) inhibitor rapamycin (a known autophagy inducer)[27,43] on the survival of starved neurons. Rapamycin elevated the percentage of cells with RFP–LC3 puncta in control neurons, but not in starved neurons (Supplementary Fig. S4d), possibly owing to a ceiling effect. Rapamycin also failed to regulate the survival of starved neurons, although it compromised neuronal survival in control neurons (Supplementary Fig. S4e). These observations collectively suggest that aberrant activation of autophagy may lead to neuronal loss, and an optimal level of autophagy is required for neuronal survival.

As starvation-induced autophagy contributes to neuronal death, we examined whether induction of autophagy led to neuronal loss in Parkinson's disease models. MPP$^+$ treatment markedly reduced neuronal survival by 48–72 h (ref. 7, Supplementary Fig. S3b). Previous

studies have demonstrated that different modes of cell death are elicited with different concentrations of MPTP (refs 12,44). To delineate the contribution of apoptosis and autophagy to MPP^+-induced neuronal loss, cultured neurons were pretreated with autophagy inhibitor 3-MA, or a pan-caspase inhibitor z-VAD-fmk, before MPP^+ treatment. Whereas z-VAD-fmk was ineffective in reducing neuronal loss, treatment with 3-MA significantly attenuated cell death induced by MPP^+ stimulation (Fig. 7a), indicating that autophagy contributed at least partially to MPP^+-induced neuronal loss. Consistent with our observation in starved neurons, whereas knockdown of Atg5 (Fig. 7b) or Atg12 (Supplementary Fig. S5c) expression slightly decreased neuronal survival in the untreated cells, MPP^+-induced neuronal loss in culture was markedly attenuated on reduction of Atg5 or Atg12 expression. These findings suggest that Atg5/Atg12-mediated autophagy is pivotal for MPP^+-induced neuronal loss. Knockdown of EndoB1 or Cdk5 expression also abrogated MPP^+-induced cell loss (Fig. 7c), which is consistent with an earlier observation that caspase-independent cell death is suppressed in EndoB1-deficient fibroblasts[30]. Furthermore, overexpression of $EndoB1^{T145A}$, but not wild-type EndoB1 or $EndoB1^{T145E}$, significantly attenuated neuronal loss triggered by MPP^+ treatment (Fig. 7d). Collectively, our observations revealed that MPTP toxicity induces autophagy-mediated neuronal loss, which is dependent on Thr 145 phosphorylation of EndoB1 by Cdk5.

Consistent with an earlier study[21], overexpression of the α-$synuclein^{A53T}$ mutant led to neuronal loss (Fig. 7e). Pretreatment with 3-MA, but not z-VAD-fmk, significantly attenuated this neuronal loss (Fig. 7e). Knockdown of Atg5 (Fig. 7f) or Atg12 (Supplementary Fig. S5d) also abrogated neuronal loss, whereas it reduced survival in vector-transfected cells (Fig. 7f and Supplementary Fig. S5d). These observations collectively suggest that autophagy induction contributes to the α-$synuclein^{A53T}$ mutant-induced neuronal loss. Importantly, we found that knockdown of EndoB1 or Cdk5 both nearly abolished this neuronal loss (Fig. 7g), and overexpression of $EndoB1^{T145A}$ significantly reduced it (Fig. 7h). Thus, Thr 145 phosphorylation of EndoB1 is critical for neuronal loss induced by overexpression of the α-$synuclein^{A53T}$ mutant.

DISCUSSION

Here we identify Cdk5 and EndoB1 as essential components in starvation-induced autophagy in neurons, in addition to revealing that elevation of Cdk5 activity leads to autophagy activation and neuronal loss in models of Parkinson's disease (Fig. 8). The significance of our findings is several-fold. First, we demonstrate the critical involvement of Cdk5 in autophagy regulation in neurons. Cdk5-mediated phosphorylation of EndoB1 at Thr 145 facilitates EndoB1 dimerization, UVRAG/Beclin 1 recruitment and autophagy induction in starved neurons. In agreement with these observations, overexpression of $EndoB1^{T145E}$, which exhibits markedly enhanced dimerization, increases the percentage of cells with RFP–LC3 puncta in Cdk5-knockdown neurons following starvation (Supplementary Fig. S6). This suggests that Thr 145 phosphorylation of EndoB1 is sufficient to trigger starvation-induced autophagy. Intriguingly, overexpression of $EndoB1^{T145E}$ fails to induce autophagy in unstarved neurons (Fig. 2f) and unstarved Cdk5-knockdown neurons (Supplementary Fig. S6). These observations suggest that, in the absence of autophagy-inducing stress, dimerization of EndoB1 alone may be insufficient to trigger

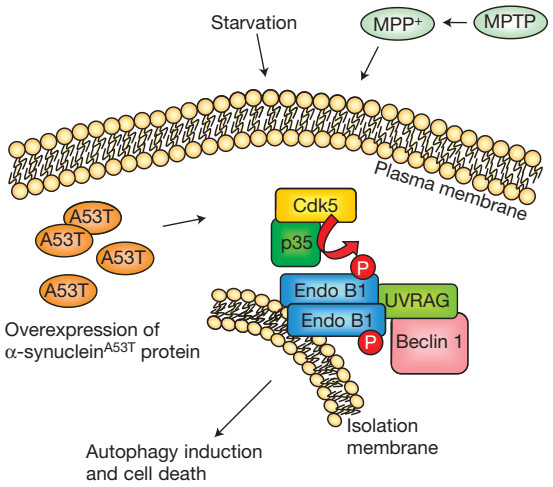

Figure 8 Proposed model for the role of Cdk5 and EndoB1 in induced autophagy and neuronal death. Cdk5-mediated Thr 145 phosphorylation of EndoB1 is required for induced autophagy and cell death in neurons. Starvation, treatment with MPTP/MPP^+ and overexpression of the α-$synuclein^{A53T}$ mutant increase the level of EndoB1 Thr 145 phosphorylation by Cdk5/p35 in neurons. Phosphorylation of EndoB1 promotes its dimerization and recruitment of the UVRAG/Beclin 1 complex to induce autophagy.

autophagy. In support of this hypothesis, elevation of Cdk5 activity through overexpression of Cdk5/p35 in HEK293T cells, which lack p35 expression and Cdk5 activity, does not increase LC3-II levels in the absence of autophagy-inducing stimuli (Supplementary Fig. S7a). Overexpression of Cdk5 or p35 in cortical neurons also fails to increase LC3-II levels, the percentage of cells exhibiting RFP–LC3 puncta or neuronal loss (Supplementary Fig. S7b–d). Taken together, our observations indicate that, although Thr 145 phosphorylation of EndoB1 by Cdk5 is required for autophagy induced by a number of autophagy-triggering stimuli, this pathway may not be sufficient to trigger autophagy in unchallenged neurons.

Our observations demonstrate that Thr 145 phosphorylation of EndoB1 is important for recruitment of UVRAG and Beclin 1. It should be noted that, although we focus on the involvement of EndoB1 and UVRAG in autophagosome formation, UVRAG is also implicated in autophagosome maturation and endocytic trafficking of epidermal growth factor receptor[38]. Interestingly, we have previously identified EndoB1 as a regulator of TrkA (high-affinity nerve growth-factor receptor) endocytic trafficking[45]. It is thus plausible that EndoB1, in combination with UVRAG, may also regulate fusion of autophagosomes with endocytic vesicles to control the degradation of autophagosome cargo. It will be interesting to further explicate the mechanisms by which autophagy is regulated by these molecules.

A second important aspect of our findings is the demonstration of autophagy regulation as a mechanism by which Cdk5 modulates neuronal loss in Parkinson's disease models. Cdk5 has been demonstrated to trigger MPTP-induced neuronal death by regulating survival factor MEF2, antioxidant enzyme Prx2 and DNA damage repair enzyme Ape1 (refs 9,13,14). Our observation not only identifies EndoB1 as an important component in Parkinson's disease pathology, but also indicates that Cdk5 activation may trigger neuronal death through multiple pathways in Parkinson's disease, underscoring the pivotal role of Cdk5 in Parkinson's disease pathophysiology. Notably, as

deregulated Cdk5 activity and abnormality in the autophagic pathway have also been observed in other neurodegenerative disorders such as Alzheimer's disease[28], the identification of Cdk5 and EndoB1 as essential components in induced autophagy raises the interesting possibility that these two proteins may also play a role in other neurodegenerative diseases through regulation of autophagy activation.

Importantly, our findings reveal autophagy deregulation as a pathophysiological mechanism of Parkinson's disease by demonstrating that autophagy is induced in Parkinson's disease models. Our evidence suggests that aberrant activation of autophagy may lead to cell loss instead of serving a protective role in Parkinson's disease. There has been a long-standing controversy concerning the precise nature of autophagy in neurodegenerative diseases. Earlier studies indicated that basal levels of chaperone-mediated autophagy and autophagy are critical for the clearance of protein aggregates and prevention of neurodegeneration[23–27]. Nonetheless, whether autophagy activation in various neurodegenerative diseases serves a protective role or a detrimental role remains incompletely understood. We have provided evidence that at least part of the cell loss can be attributed to the autophagic pathway, revealing a pathological role of aberrant autophagy activation. Interestingly, similar observations have been obtained in starved neurons, suggesting that aberrant autophagy activation induced by other stressors may also result in neuronal loss. In addition, as rapamycin also compromises neuronal survival in unstarved cells, our findings raise the need to re-examine the use of autophagy activators as therapeutic agents against Parkinson's disease, and indicate that maintaining autophagy at an optimal level might be the key to attenuating neuronal loss in Parkinson's disease. As Cdk5-mediated phosphorylation of EndoB1 is required for autophagy induced by several stressors, but has a negligible effect on basal autophagy, our findings suggest that this pathway may be selectively activated under pathological conditions. Indeed, inhibition of the Cdk5/EndoB1-mediated signalling attenuates only pathological autophagy activation and neuronal loss, while sparing the basal level of autophagy that is critical for neuronal function and survival. The identification of pathways that are selectively activated during pathological conditions also suggests that different machinery may be implicated in the control of basal and induced autophagy under pathological conditions. In support of this hypothesis, a recent study identified the engulfment receptor Draper as a factor that is selectively involved in autophagy activation during cell death[46]. It will be interesting to further delineate the molecular mechanisms implicated in the control of basal and induced/pathological autophagy, which will provide important insights for the development of selective autophagy inhibitors as therapeutics for Parkinson's disease. □

METHODS

Methods and any associated references are available in the online version of the paper at http://www.nature.com/naturecellbiology/

Note: Supplementary Information is available on the Nature Cell Biology website

ACKNOWLEDGEMENTS

We are grateful to A. B. Kulkarni (National Institutes of Health, USA) and T. Curran (St Jude Children's Research Hospital, USA) for the *Cdk5*-knockout mice. *p35*-knockout mice were provided by L. H. Tsai (Massachusetts Institute of Technology, USA). We thank T. Yoshimori (Osaka University, Japan) for the mRFP–LC3 construct, V. M. Y. Lee (University of Pennsylvania School of Medicine, USA) for the SNL-1 antibody and wild-type α-synuclein and α-synuclein^{A53T} constructs and J. Yuan (Harvard Medical School) for the pcDNA3-Beclin 1 construct. We thank J. Li, G. Ke, W. Y. Fu, K. Cheng, J. Wan, Y. P. Ng, V. Lee and A. Lai for technical assistance, and members of the Ip laboratory for discussions. This work was supported in part by the Research Grants Council of Hong Kong (HKUST 661007, 661109, 660309, 660210, 1/06C and 6/CRF/08), the Area of Excellence Scheme of the University Grants Committee (AoE/B-15/01) and the Hong Kong Jockey Club. N.Y.I. and Z.H.C. were recipients of the Croucher Foundation Senior Research Fellowship and Croucher Foundation Fellowship, respectively.

AUTHOR CONTRIBUTIONS

A.S.L.W., R.H.K.L., A.Y.C. and P.K.Y. carried out the experiments. A.S.L.W., R.H.K.L., A.Y.C., P.K.Y., Z.H.C. and N.Y.I. planned the studies, designed the experiments and interpreted the results. S.K.C., Z.H.C. and N.Y.I. provided reagents and resources. A.S.L.W., Z.H.C. and N.Y.I. wrote the manuscript. All authors discussed the results and commented on the manuscript.

COMPETING FINANCIAL INTERESTS

The authors declare no competing financial interests.

Published online at http://www.nature.com/naturecellbiology
Reprints and permissions information is available online at http://npg.nature.com/reprintsandpermissions/

1. Dhavan, R. & Tsai, L. H. A decade of CDK5. *Nat. Rev. Mol. Cell Biol.* **2,** 749–759 (2001).
2. Cheung, Z. H., Fu, A. K. & Ip, N. Y. Synaptic roles of Cdk5: implications in higher cognitive functions and neurodegenerative diseases. *Neuron* **50,** 13–18 (2006).
3. Cheung, Z. H. & Ip, N. Y. Cdk5: mediator of neuronal death and survival. *Neurosci. Lett.* **361,** 47–51 (2004).
4. Cheung, Z. H., Gong, K. & Ip, N. Y. Cyclin-dependent kinase 5 supports neuronal survival through phosphorylation of Bcl-2. *J. Neurosci.* **28,** 4872–4877 (2008).
5. Li, B. S. *et al.* Cyclin-dependent kinase 5 prevents neuronal apoptosis by negative regulation of c-Jun N-terminal kinase 3. *EMBO J.* **21,** 324–333 (2002).
6. O'Hare, M. J. *et al.* Differential roles of nuclear and cytoplasmic cyclin-dependent kinase 5 in apoptotic and excitotoxic neuronal death. *J. Neurosci.* **25,** 8954–8966 (2005).
7. Smith, P. D. *et al.* Cyclin-dependent kinase 5 is a mediator of dopaminergic neuron loss in a mouse model of Parkinson's disease. *Proc. Natl Acad. Sci. USA* **100,** 13650–13655 (2003).
8. Patrick, G. N. *et al.* Conversion of p35 to p25 deregulates Cdk5 activity and promotes neurodegeneration. *Nature* **402,** 615–622 (1999).
9. Smith, P. D. *et al.* Calpain-regulated p35/cdk5 plays a central role in dopaminergic neuron death through modulation of the transcription factor myocyte enhancer factor 2. *J. Neurosci.* **26,** 440–447 (2006).
10. Paoletti, P. *et al.* Dopaminergic and glutamatergic signalling crosstalk in Huntington's disease neurodegeneration: the role of p25/cyclin-dependent kinase 5. *J. Neurosci.* **28,** 10090–10101 (2008).
11. Dauer, W. & Przedborski, S. Parkinson's disease: mechanisms and models. *Neuron* **39,** 889–909 (2003).
12. Levy, O. A., Malagelada, C. & Greene, L. A. Cell death pathways in Parkinson's disease: proximal triggers, distal effectors, and final steps. *Apoptosis* **14,** 478–500 (2009).
13. Qu, D. *et al.* Role of Cdk5-mediated phosphorylation of Prx2 in MPTP toxicity and Parkinson's disease. *Neuron* **55,** 37–52 (2007).
14. Huang, E. *et al.* The role of Cdk5-mediated apurinic/apyrimidinic endonuclease 1 phosphorylation in neuronal death. *Nat. Cell Biol.* **12,** 563–571 (2010).
15. Rubinsztein, D. C. The roles of intracellular protein-degradation pathways in neurodegeneration. *Nature* **443,** 780–786 (2006).
16. Maiuri, M. C., Zalckvar, E., Kimchi, A. & Kroemer, G. Self-eating and self-killing: crosstalk between autophagy and apoptosis. *Nat. Rev. Mol. Cell Biol.* **8,** 741–752 (2007).
17. Zhu, J. H., Guo, F., Shelburne, J., Watkins, S. & Chu, C. T. Localization of phosphorylated ERK/MAP kinases to mitochondria and autophagosomes in Lewy body diseases. *Brain Pathol.* **13,** 473–481 (2003).
18. Anglade, P. *et al.* Apoptosis and autophagy in nigral neurons of patients with Parkinson's disease. *Histol. Histopathol.* **12,** 25–31 (1997).
19. Zhu, J. H. *et al.* Regulation of autophagy by extracellular signal-regulated protein kinases during 1-methyl-4-phenylpyridinium-induced cell death. *Am. J. Pathol.* **170,** 75–86 (2007).
20. Stefanis, L., Larsen, K. E., Rideout, H. J., Sulzer, D. & Greene, L. A. Expression of A53T mutant but not wild-type α-synuclein in PC12 cells induces alterations of the ubiquitin-dependent degradation system, loss of dopamine release, and autophagic cell death. *J. Neurosci.* **21,** 9549–9560 (2001).
21. Xilouri, M., Vogiatzi, T., Vekrellis, K., Park, D. & Stefanis, L. Aberrant α-synuclein confers toxicity to neurons in part through inhibition of chaperone-mediated autophagy. *PloS One* **4,** e5515 (2009).
22. Cheung, Z. H. & Ip, N. Y. The emerging role of autophagy in Parkinson's disease. *Mol. Brain* **2,** 29 (2009).

23. Cuervo, A. M., Stefanis, L., Fredenburg, R., Lansbury, P. T. & Sulzer, D. Impaired degradation of mutant α-synuclein by chaperone-mediated autophagy. *Science* **305,** 1292–1295 (2004).
24. Vogiatzi, T., Xilouri, M., Vekrellis, K. & Stefanis, L. Wild type α-synuclein is degraded by chaperone-mediated autophagy and macroautophagy in neuronal cells. *J. Biol. Chem.* **283,** 23542–23556 (2008).
25. Hara, T. *et al.* Suppression of basal autophagy in neural cells causes neurodegenerative disease in mice. *Nature* **441,** 885–889 (2006).
26. Komatsu, M. *et al.* Loss of autophagy in the central nervous system causes neurodegeneration in mice. *Nature* **441,** 880–884 (2006).
27. Ravikumar, B. *et al.* Inhibition of mTOR induces autophagy and reduces toxicity of polyglutamine expansions in fly and mouse models of Huntington disease. *Nat. Genet.* **36,** 585–595 (2004).
28. Levine, B. & Kroemer, G. Autophagy in the pathogenesis of disease. *Cell* **132,** 27–42 (2008).
29. Yang, Q. *et al.* Regulation of neuronal survival factor MEF2D by chaperone-mediated autophagy. *Science* **323,** 124–127 (2009).
30. Takahashi, Y. *et al.* Bif-1 interacts with Beclin 1 through UVRAG and regulates autophagy and tumourigenesis. *Nat. Cell Biol.* **9,** 1142–1151 (2007).
31. Modregger, J., Schmidt, A. A., Ritter, B., Huttner, W. B. & Plomann, M. Characterization of endophilin B1b, a brain-specific membrane-associated lysophosphatidic acid acyl transferase with properties distinct from endophilin A1. *J. Biol. Chem.* **278,** 4160–4167 (2003).
32. Farsad, K. *et al.* Generation of high curvature membranes mediated by direct endophilin bilayer interactions. *J. Cell Biol.* **155,** 193–200 (2001).
33. Cuddeback, S. M. *et al.* Molecular cloning and characterization of Bif-1. A novel Src homology 3 domain-containing protein that associates with Bax. *J. Biol. Chem.* **276,** 20559–20565 (2001).
34. Gallop, J. L. *et al.* Mechanism of endophilin N-BAR domain-mediated membrane curvature. *EMBO J.* **25,** 2898–2910 (2006).
35. Klionsky, D. J. *et al.* Guidelines for the use and interpretation of assays for monitoring autophagy in higher eukaryotes. *Autophagy* **4,** 151–175 (2008).
36. Mizushima, N., Yoshimori, T. & Levine, B. Methods in mammalian autophagy research. *Cell* **140,** 313–326 (2010).
37. Huttner, W. B. & Schmidt, A. A. Membrane curvature: a case of endofeelin. *Trends Cell Biol.* **12,** 155–158 (2002).
38. Liang, C. *et al.* Beclin1-binding UVRAG targets the class C Vps complex to coordinate autophagosome maturation and endocytic trafficking. *Nat. Cell Biol.* **10,** 776–787 (2008).
39. Liang, C. *et al.* Autophagic and tumour suppressor activity of a novel Beclin1-binding protein UVRAG. *Nat. Cell Biol.* **8,** 688–699 (2006).
40. Martin, L. J. *et al.* Parkinson's disease α-synuclein transgenic mice develop neuronal mitochondrial degeneration and cell death. *J. Neurosci.* **26,** 41–50 (2006).
41. Giasson, B. I. *et al.* Neuronal α-synucleinopathy with severe movement disorder in mice expressing A53T human α-synuclein. *Neuron* **34,** 521–533 (2002).
42. Mizushima, N., Levine, B., Cuervo, A. M. & Klionsky, D. J. Autophagy fights disease through cellular self-digestion. *Nature* **451,** 1069–1075 (2008).
43. Schmelzle, T. & Hall, M. N. TOR, a central controller of cell growth. *Cell* **103,** 253–262 (2000).
44. Bredesen, D. E., Rao, R. V. & Mehlen, P. Cell death in the nervous system. *Nature* **443,** 796–802 (2006).
45. Wan, J. *et al.* Endophilin B1 as a novel regulator of nerve growth factor/ TrkA trafficking and neurite outgrowth. *J. Neurosci.* **28,** 9002–9012 (2008).
46. McPhee, C. K., Logan, M. A., Freeman, M. R. & Baehrecke, E. H. Activation of autophagy during cell death requires the engulfment receptor Draper. *Nature* **465,** 1093–1096 (2010).

DOI: 10.1038/ncb2217

METHODS

Plasmids and RNA interference. The expression vector of mRFP–LC3 was a gift from T. Yoshimori (Osaka University, Japan). Wild-type α-synuclein and α-synuclein^{A53T} constructs were gifts from V. M. Y. Lee (University of Pennsylvania School of Medicine, USA). pcDNA3-Beclin 1 construct (no. 21150) was obtained from Addgene[47]. The pCMV-SPORT6 vector of UVRAG was obtained from Invitrogen. The pcDNA3 vectors of p35, Cdk5 and EndoB1 were prepared as previously described[45,48,49]. The last 30 nucleotides of *EndoB1* are absent from the truncated EndoB1 construct. EndoB1 mutants were constructed by mutating Thr 145, Thr 269 or both to alanine or glutamic acid using the overlapping PCR technique. The EndoB1 5E mutant was prepared by mutating Lys 176, Arg 178, Lys 180, Lys 181 and Lys 183 residues to glutamic acid. GFP-, HA- and GST-tagged EndoB1 constructs were generated by subcloning the *EndoB1* sequence into expression vectors pEGFP-N1, pcDNA3-HA (Invitrogen) and pGEX-6P-1 (Amersham-Biosciences), respectively. The Flag-tag sequence was inserted into EndoB1 constructs by the standard PCR technique. For gene knockdown by RNA interference (RNAi), pSUPER vector-based small hairpin RNAs of *EndoB1*, *Cdk5*, *Atg5* and *Atg12* were constructed as previously described[45,48,50]. The RNAi target sense sequence for EndoB1 is 5′-AAGCTGCAGAAACTAAAAG-3′, that for Cdk5 is 5′-TGCCACGGGGAGAGACCTG-3′, that for Atg5 is 5′-ATCTGAGCTATCCAGACAA-3′ and that for Atg12 is 5′-GGGACGTGCATAGTT-TAAA-3′.

Antibodies. The antibody against α-synuclein (SNL-1) was a gift from V. M. Y. Lee (University of Pennsylvania School of Medicine, USA). Other antibodies used include anti-GST (1:1,000; Amersham-Biosciences), anti-HA (1:1,000; Roche Applied Science), anti-Atg12 (1:2,000; C18, Santa Cruz Biotechnology), anti-Cdk5 (1:1,000; C8 and DC17, Santa Cruz Biotechnology), anti-p35 (1:1,000; C-19, Santa Cruz Biotechnology), anti-EndoB1 (1:1,000; Imgenex), anti-tyrosine hydroxylase (1:1,000; Imgenex), anti-Atg5 (1:1,000; Novus Biologicals), anti-UVRAG (1:1,000; Sigma-Aldrich), anti-α-tubulin (1:10,000; Sigma-Aldrich), anti-β-actin (1:10,000; Sigma-Aldrich), antiphospho-Thr-Pro (1:1,000; Cell Signaling Technology), anti-GFP (1:1,000; Cell Signaling Technology), anti-LC3B (1:1,000; Cell Signaling Technology) and anti-Beclin 1 (1:1,000; Cell Signaling Technology). Anti-phospho-Thr145-EndoB1 antibody was raised in rabbit immunized with a synthetic peptide encoding the 141–155 amino acids of EndoB1 (CNFLTPLRN-FIEGDY; Invitrogen), and was purified from serum using SulfoLink Coupling Gel (Pierce).

Animals. Sprague Dawley rats and C57BL/6 mice were used in this study. *Cdk5*-knockout mice were provided by A. B. Kulkarni (National Institutes of Health, USA) and T. Curran (St Jude Children's Research Hospital, USA). *p35*-knockout mice were provided by L. H. Tsai (Massachusetts Institute of Technology, USA). α-synuclein^{A53T} transgenic mice were obtained from The Jackson Laboratory. Mice were collected at the desired stage and genotyped.

MPTP administration. MPTP was administrated to 10-week-old male mice (26–31 g) as previously reported[7]. In brief, a single injection of 25 mg kg^{-1} 1-methyl-4-phenyl-1,2,3,6-tetrahydropyridine (MPTP.HCl, Research Biochemicals International) was administered subcutaneously to the mice daily for five consecutive days. An equivalent volume of 0.9% saline was used as the vehicle. Mice were killed at days 0, 1, 3 and 5 after the last injection. The brain was dissected for protein extraction or fixed in 10% formalin (BDH, VWR international) for further immunohistochemical study.

Primary neuron cultures and transfection. Primary cortical neuron cultures were prepared from rat embryos at E18 and maintained as previously described[48,49]. Neurons were transfected with a primary neuron nucleofection kit (Amaxa Biosystems) according to the manufacturer's instructions before cell plating. Alternatively, neurons were plated and transfected at 3–5 days *in vitro* using calcium phosphate precipitation. To starve the neurons, cells were washed once with Earle's Balanced Salt Solution (Sigma-Aldrich), and then cultured with Earle's Balanced Salt Solution for 3 h. For treatment with 1-methyl-4-phenylpyridinium (MPP^+), 20 μM MPP^+ (Sigma-Aldrich) was added to the neuron cultures for 16 h for assessment of autophagy induction, and 72 h for quantification of cell viability. Autophagy induction and neuronal survival in cells expressing the α-synuclein^{A53T} mutant were quantified at day 5 after transfection. In some experiments, cultured neurons were treated with 10 mM 3-MA, 10 μg ml^{-1} E64d, 10 μg ml^{-1} pepstatin A (Sigma-Aldrich), 20 μM z-VAD-fmk (Promega), 10 nM rapamycin or 10 μM roscovitine (Calbiochem) for 30 min before starvation, 1 h before treatment with MPP^+ or 1 day after transfection of α-synuclein.

Cell cultures and transfection. HEK293T and COS-7 cells were obtained from the American Type Culture Collection. HEK293T and COS-7 cells were cultured in DMEM supplemented with 10% heat-inactivated fetal bovine serum, penicillin (50 units ml^{-1}) and streptomycin (100 μg ml^{-1}) at 37 °C in a humidified atmosphere with 5% CO_2. HEK293T and COS-7 cells were transfected with Lipofectamine Plus transfection reagents (Invitrogen) according to the manufacturer's instructions.

Protein extraction, immunoprecipitation, *in vitro* pulldown assay and immunoblot analysis. Protein extraction, fractionation of membrane and cytosolic proteins, gel filtration assay, *in vitro* pulldown assay, *in vitro* kinase assay, immunoprecipitation and immunoblotting were carried out as previously described[49,51,52]. Briefly, 500 μg–2 mg of protein lysate was incubated with 1–2 μg of the corresponding antibody at 4 °C overnight with end-to-end rotation for immunoprecipitation. The antibody was pulled down by incubation with protein G-Sepharose beads (Amersham Biosciences). For *in vitro* pulldown assays, GST fusion proteins were expressed in *Escherichia coli* (BL21 strain) and purified using a glutathione-Sepharose 4B column according to the manufacturer's instructions (GE Healthcare). Purified GST fusion protein was incubated with cell lysate expressing the desired protein, followed by pulldown using glutathione-Sepharose beads (GE Healthcare). The bound proteins were subjected to SDS–PAGE and immunoblot analysis.

Lipid-binding assay. GST fusion proteins of EndoB1 were expressed in *E. coli* (BL21 strain) and purified using a glutathione-Sepharose 4B column according to the manufacturer's instructions (GE Healthcare). GST was cleaved from the fusion proteins using PreScission protease (GE Healthcare). The lipid-binding assay was carried out as previously described[53]. The supernatant fraction with proteins unbound to lipids was collected, and the pellet fraction with proteins bound to lipids was washed once and resuspended in the same volume of buffer as for the supernatant fraction. The supernatant and pellet fractions were subjected to SDS–PAGE and the proteins were visualized by GelCode Blue Stain Reagent (Thermo Scientific).

Immunohistochemistry. Serial sagittal paraffin sections (7 μm) were rehydrated in 0.3% hydrogen peroxide (VWR Laboratory Supplies) to block any endogenous peroxidase activity. The sections were then blocked with 1.5% normal goat serum for 1 h at room temperature, and incubated with antibody against tyrosine hydroxylase at 4 °C overnight. Immunoreactivity was detected with biotinylated secondary antibodies and visualized with a Vectastain Elite ABC Kit (Vector Laboratories) with 3,3′-diaminobenzidine tetrahydrochloride (Liquid DAB substrate kit, Zymed). Harris haematoxylin was used as the counterstain of the nucleus. To quantify neuronal survival in the substantia nigra, sections adjacent to the ones used for tyrosine hydroxylase staining were stained with cresyl violet. Photomicrographs were taken with a light microscope system (Zeiss) and the analysis was made in a blinded fashion. The number of tyrosine hydroxylase-positive and cresyl violet-stained neurons in the substantia nigra was counted systematically under a light microscope with the aid of Neurolucida 8.0 software. For each experimental animal, a total of three sections approximately 80 μm apart was used.

Fluorescence microscopy. To visualize RFP–LC3 puncta, cells were fixed with 4% paraformaldehyde in PBS at room temperature for 10 min, washed with PBS and mounted on slides with a Prolong Antifade kit (Invitrogen). Cells were observed under a fluorescence microscope (Olympus). The percentage of neurons showing accumulation of RFP–LC3 puncta (that is with at least five puncta per neuron) was quantified. For immunofluorescence study, cells were fixed with 3% paraformaldehyde in PBS at room temperature for 5 min, and then with 100% methanol for 5 min at −20 °C. Cells were washed with 75% methanol/PBS, 50% methanol/PBS and 25% methanol/PBS and twice with PBS, blocked and permeabilized with 1% BSA, 0.4% Triton X-100 in PBS for 30 min at room temperature and incubated with antibodies against Atg5 at 4 °C overnight. Immunoreactivity was detected with the Alexa Fluor dye-conjugated secondary antibodies (Invitrogen) and visualized under a fluorescence microscope (Olympus).

Cell viability assay. Cell viability was determined by SYTOX Green uptake assay and MTT (3-(4,5-dimethylthiazol-2-yl)-2,5-diphenyltetrazolium bromide) assay. Cortical neurons were treated with 1 μM SYTOX Green (Invitrogen) for 10 min and washed with PBS three times. The cells were then fixed with 3% paraformaldehyde in PBS for 5 min at room temperature, mounted and visualized as described above. Cells with green fluorescent signal were counted as positive for cell death. At least 50 cells were counted for each experimental condition. Each experiment was repeated at least three times. Alternatively, MTT solution was added to the neuronal cultures in a 48-well plate at a 1:10 volume ratio to the medium and incubated at 37 °C with 5% CO_2 for 4 h. Viable cells convert the soluble MTT salt to insoluble blue formazan crystals. Formazan crystals formed were dissolved with solubilization buffer at 37 °C overnight. The absorbance of the solubilized formazan

was measured at 570 nm using a microplate reader. Each experiment was repeated at least three times.

Statistical analysis. All data were presented as the mean ± s.em. Statistical analysis was determined by an unpaired Student *t*-test or one-way analysis of variance (ANOVA) followed by Bonferroni's *post hoc* test. A P value of less than 0.05 was considered statistically significant. $^{*}P < 0.05$; $^{**}P < 0.01$; $^{***}P < 0.001$.

47. Shibata, M. *et al*. Regulation of intracellular accumulation of mutant Huntingtin by Beclin 1. *J. Biol. Chem.* **281,** 14474–14485 (2006).
48. Fu, W. Y. *et al*. Cdk5 regulates EphA4-mediated dendritic spine retraction through an ephexin1-dependent mechanism. *Nat. Neurosci.* **10,** 67–76 (2007).
49. Cheung, Z. H., Chin, W. H., Chen, Y., Ng, Y. P. & Ip, N. Y. Cdk5 is involved in BDNF-stimulated dendritic growth in hippocampal neurons. *PLoS Biol.* **5,** e63 (2007).
50. Lee, J. A. & Gao, F. B. Inhibition of autophagy induction delays neuronal cell loss caused by dysfunctional ESCRT-III in frontotemporal dementia. *J. Neurosci.* **29,** 8506–8511 (2009).
51. Cheng, K. *et al*. Pctaire1 interacts with p35 and is a novel substrate for Cdk5/p35. *J. Biol. Chem.* **277,** 31988–31993 (2002).
52. Lai, K. O. *et al*. Identification of the Jak/Stat proteins as novel downstream targets of EphA4 signalling in muscle: implications in the regulation of acetylcholinesterase expression. *J. Biol. Chem.* **279,** 13383–13392 (2004).
53. Jin, W. *et al*. Lipid binding regulates synaptic targeting of PICK1, AMPA receptor trafficking, and synaptic plasticity. *J. Neurosci.* **26,** 2380–2390 (2006).

nature cell biology

DOI: 10.1038/ncb2217

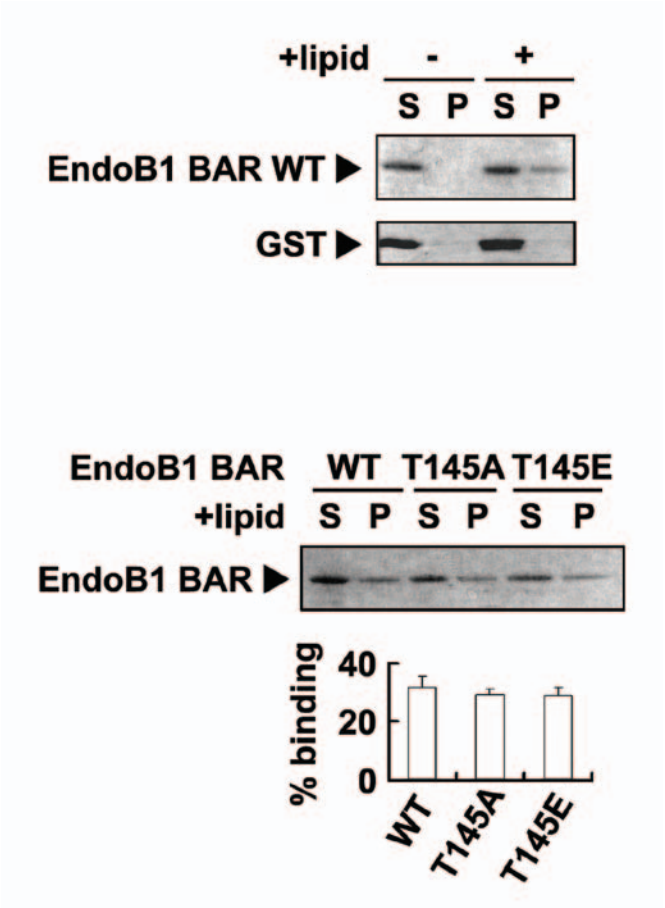

Figure S1 Thr145 phosphorylation of EndoB1 negligibly affected lipid binding of the N-BAR domain of EndoB1. Purified wild type, T145A or T145E mutant of the N-BAR domain of EndoB1 were incubated with brain lipid extracts. Purified GST protein was included as a negative control. S = supernatant fraction; P = pellet fraction that contains the lipid-bound proteins. Data are means ± s.e.m.; n = 3.

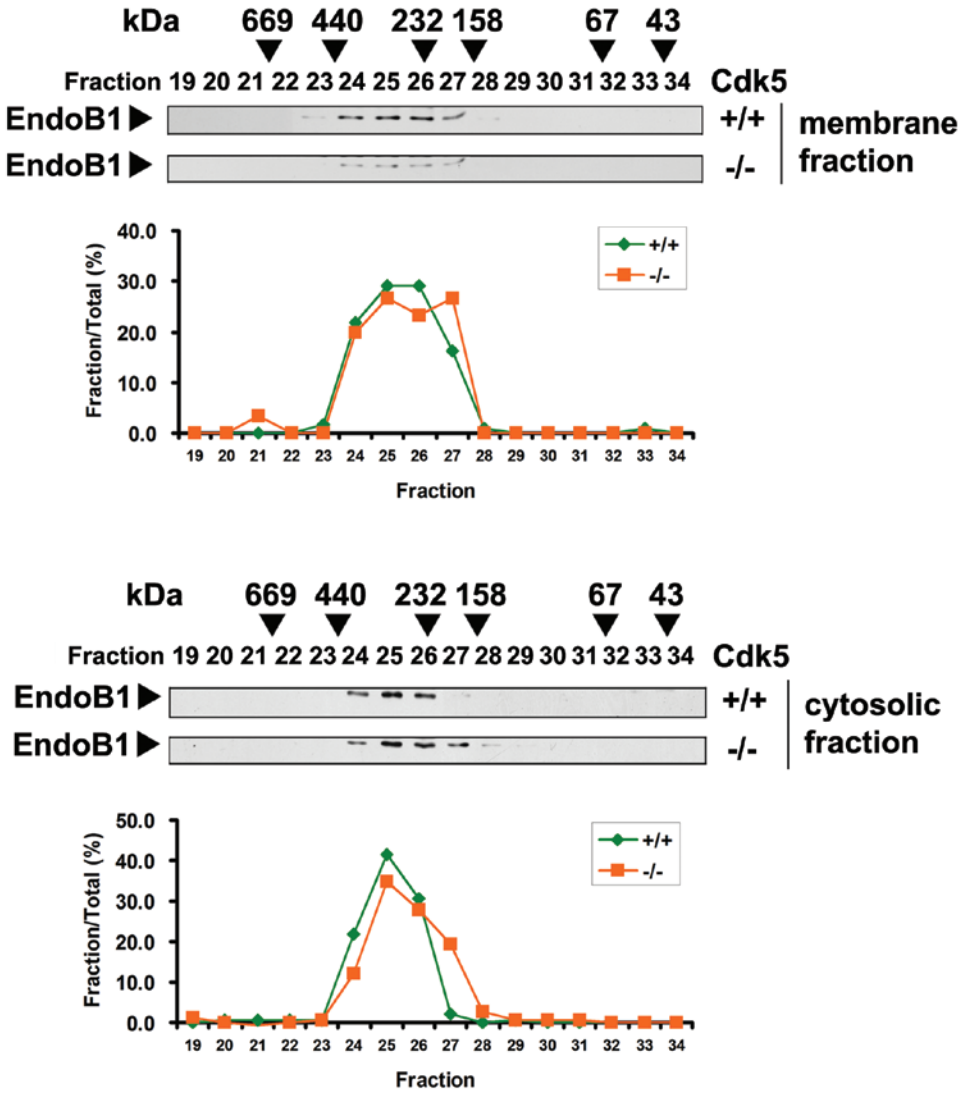

Figure S2 Altered membrane/cytosolic distribution of EndoB1 in Cdk5-deficient mice brain. Gel filtration analysis of the membrane and cytosolic fractions of $Cdk5^{+/+}$ and $Cdk5^{-/-}$ mice brain lysates. Protein fractions were immunoblotted with antibody against EndoB1. Relative amount of EndoB1 in each fraction was determined and plotted.

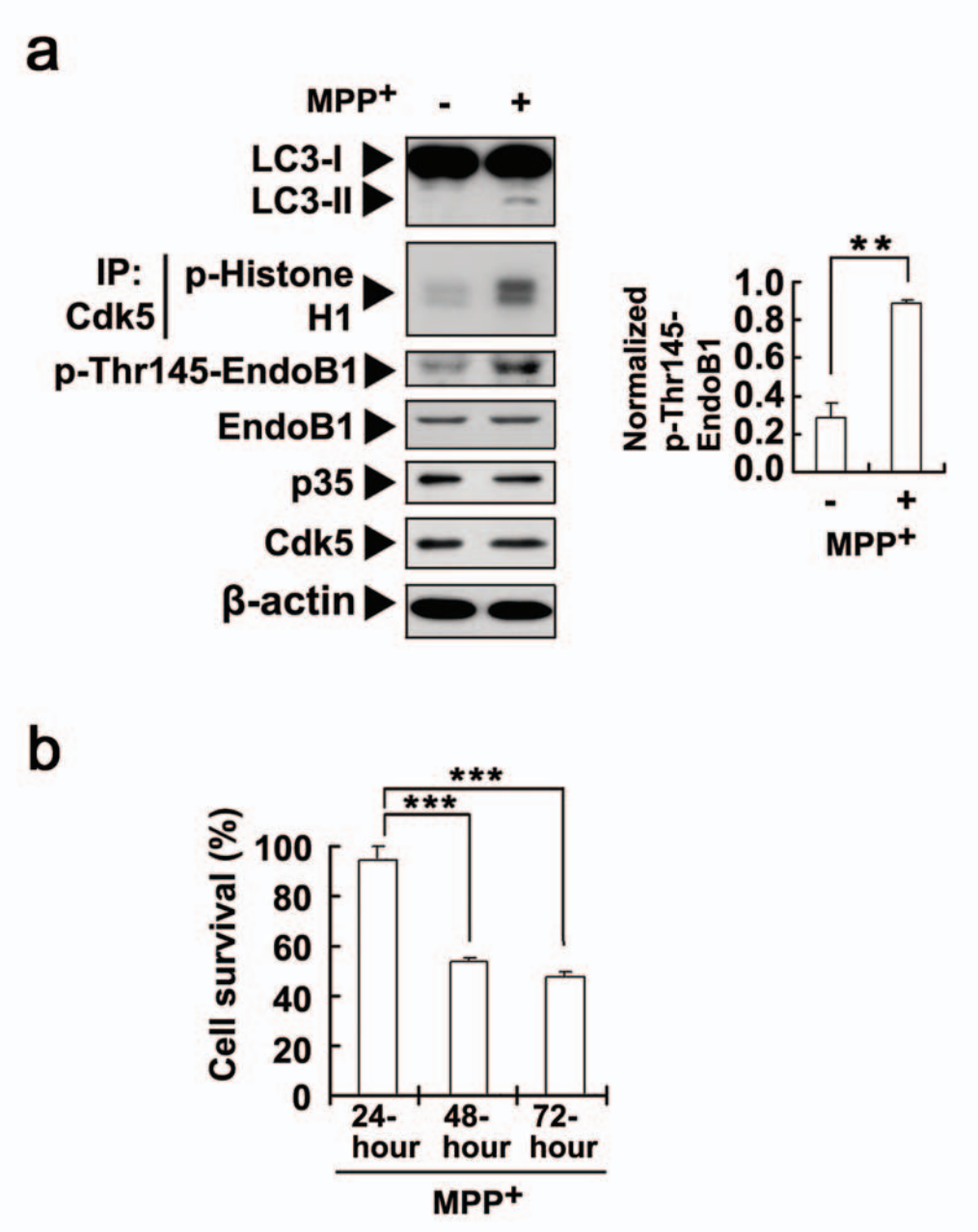

Figure S3 MPP+ treatment increases LC3-II level, Cdk5 kinase activity, Thr145-phosphorylated EndoB1, and cell death in neurons. **a,** Cortical neurons were either untreated or treated with 20 μM of MPP+ for 16 hrs. Protein lysates were immunoblotted with indicated antibodies or immunoprecipitated with antibody for Cdk5. The immunoprecipitates were then subjected to *in vitro* kinase assay. Data are means ± s.e.m.; n = 3. **b**, MPP+ treatment induces cell death in cortical neurons. Cortical neurons were treated with 20 μM of MPP+ for indicated time periods and the viability of neurons was measured by MTT assay. The percentage of cell survival was obtained by comparing value from the MPP+-treated neurons to that of the untreated ones. Data are means ± s.e.m.; n = 4.

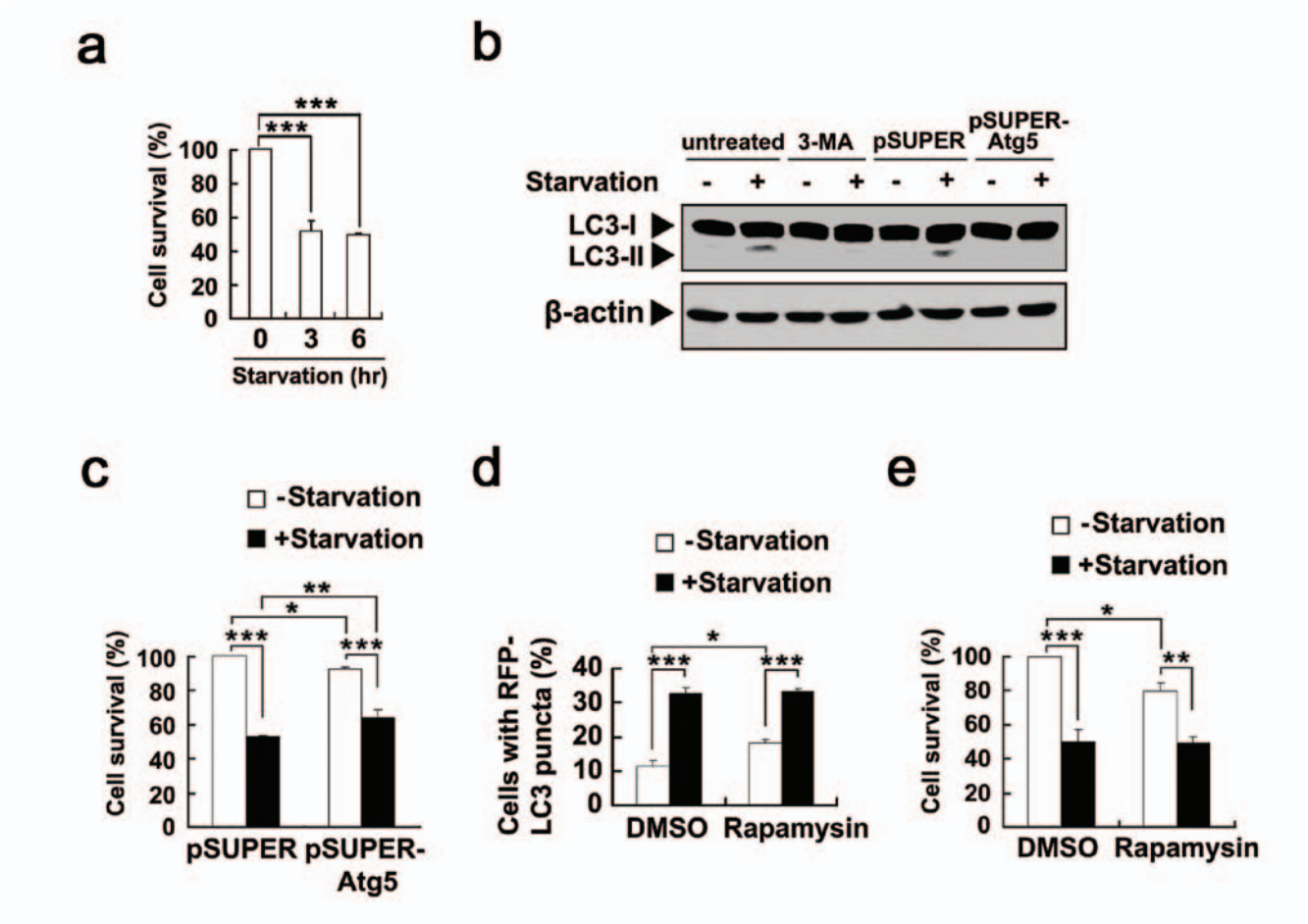

Figure S4 Autophagy contributes to neuronal loss in starved neurons. **a,** Starvation induces neuronal death in cortical neurons as quantified by MTT assay. Data are means ± s.e.m.; n = 4. **b,** Knock-down of Atg5 expression and 3-MA treatment both reduce LC3-II levels in starved neurons. **c,** Knock-down of Atg5 expression inhibits starvation-induced neuronal loss, while reducing survival of untreated neurons. Data are means ± s.e.m.; n = 3. **d, e,** Pre-treatment with 10 nM of rapamycin increases the level of RFP-LC3 puncta (d) and cell death (e) in untreated neurons, but not in starved neurons. Data are means ± s.e.m.; n = 3 for (**d**) and n = 6 for (**e**).

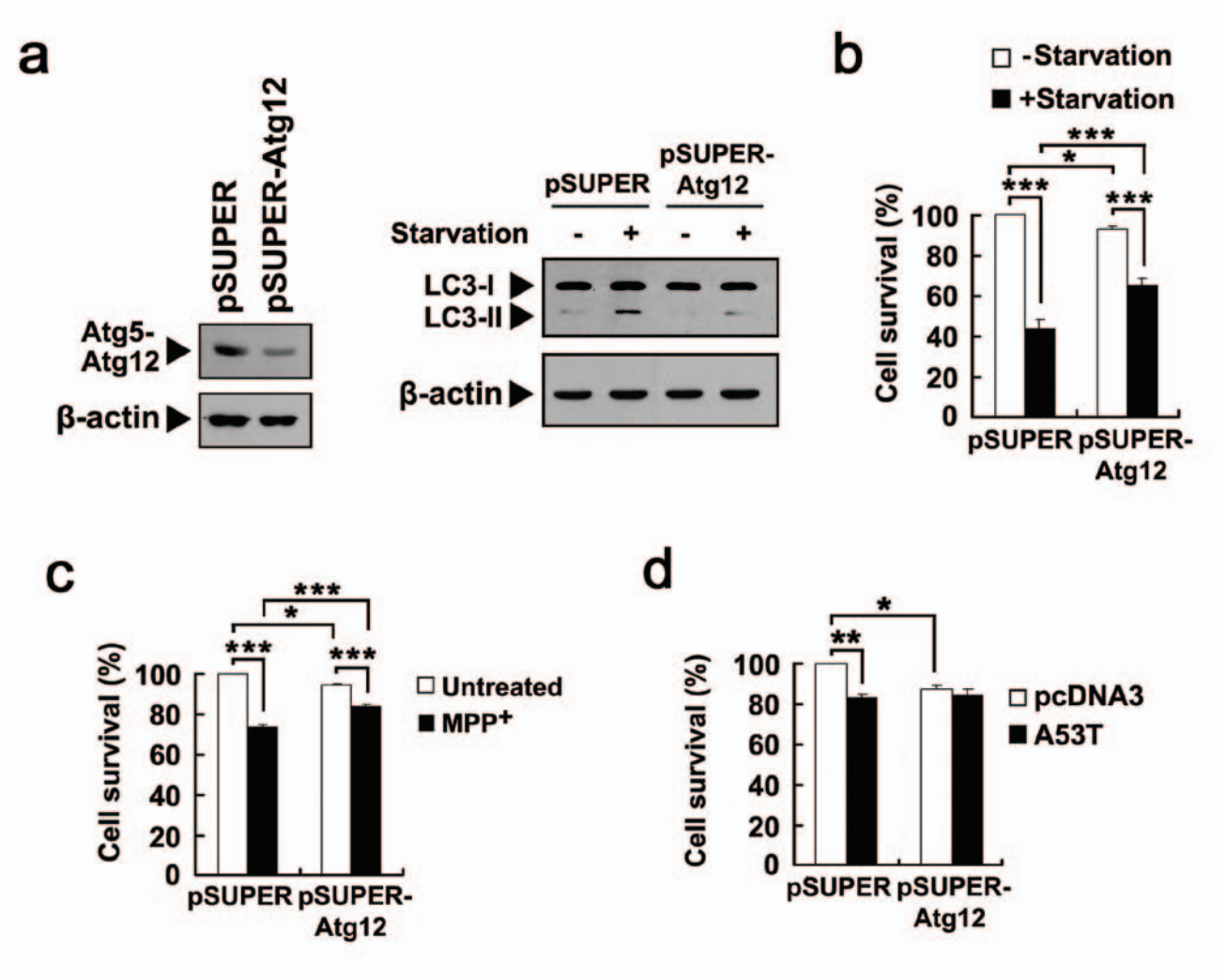

Figure S5 Knock-down of Atg12 inhibits reduces neuronal death in starved, MPP^+-treated and A53T alpha-synuclein mutant-expressing neurons. **a,** Knock-down of Atg12 expression reduces the level of LC3-II in cultured cortical neurons. **b-d,** Knock-down of Atg12 expression inhibits neuronal loss induced by starvation (b), MPP^+ (c) and A53T alpha-synuclein mutant overexpression (d), but causes death in untreated neurons. Data are means ± s.e.m.; n = 6 for (**b**) and n = 3 for (**c, d**).

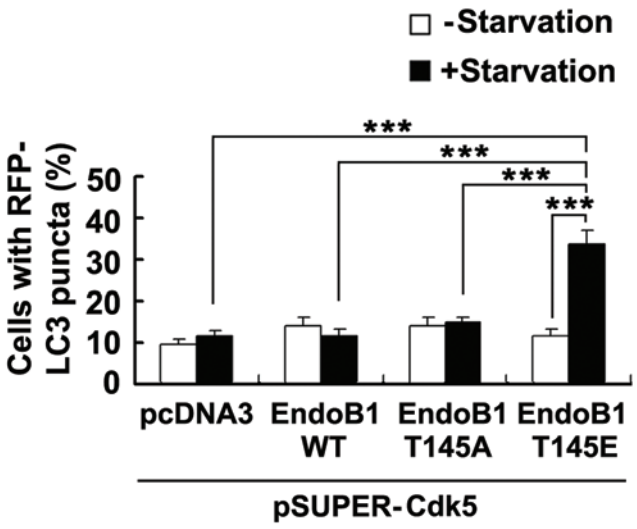

Figure S6 Overexpression of T145E EndoB1 promotes starvation-induced autophagy in Cdk5-knocked-down neurons. Rat cortical neurons transfected with RFP-LC3, pSUPER-Cdk5 and the indicated EndoB1 constructs were starved in EBSS medium for 3 hours, and the percentage of neurons with RFP-LC3 puncta was counted. Data are means ± s.e.m.; n = 3.

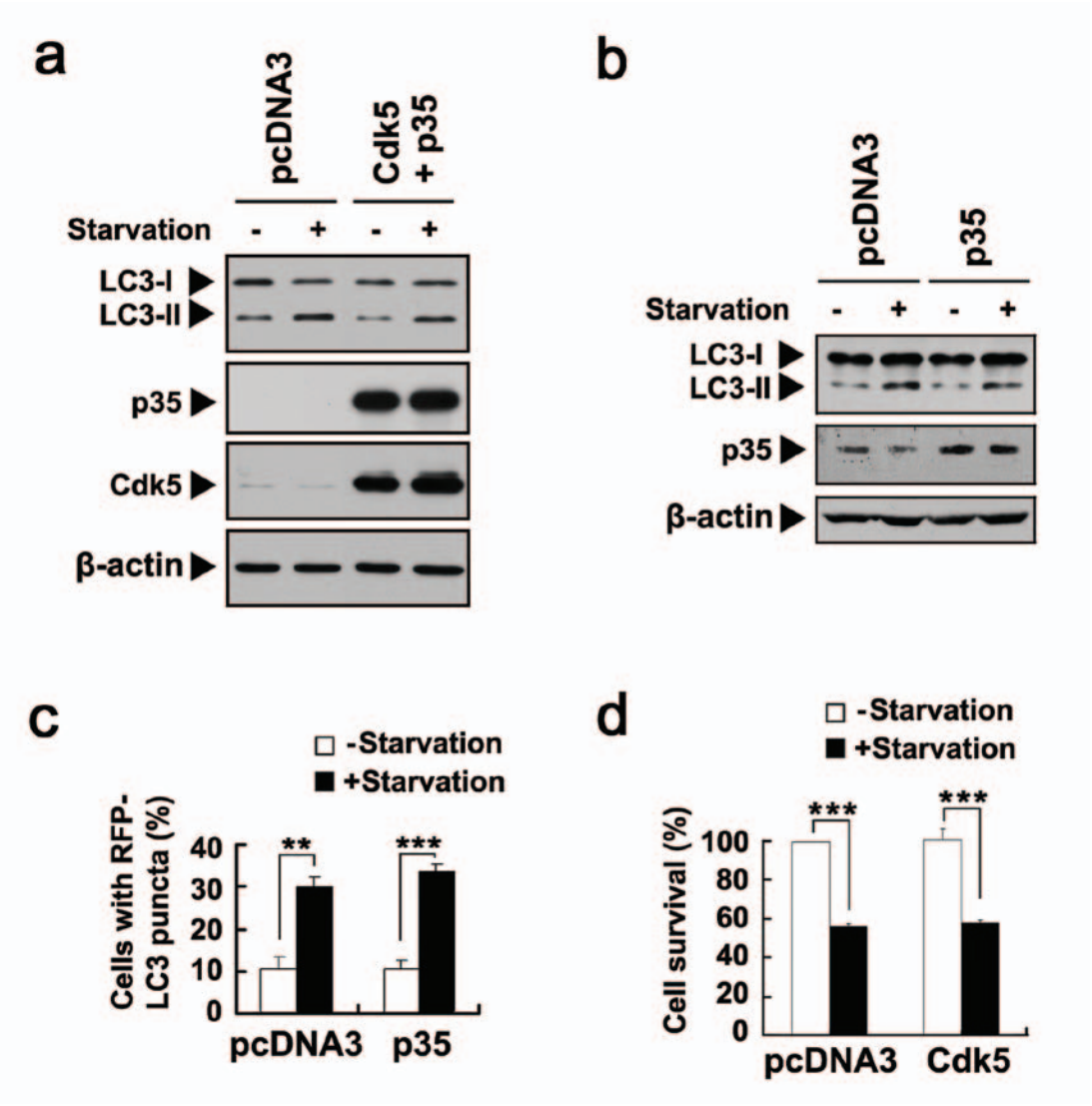

Figure S7 Cdk5 and/or p35 overexpression is not sufficient to induce autophagy and neuronal death. **a,** Overexpression of Cdk5/p35 does not affect LC3-II levels in starved 293T cells following incubation with EBSS for 3 hours. **b, c,** Overexpression of p35 does not affect basal or starvation-induced increase in LC3-II level (**b**) and level of RFP-LC3 puncta (**c**) in cortical neurons. Data are means ± s.e.m.; n = 3. Similar results were obtained with Cdk5 overexpression. **d,** Overexpression of Cdk5 has negligible effects on the survival of control or starved cortical neurons. Data are means ± s.e.m.; n = 3. Similar results were obtained with p35 overexpression.

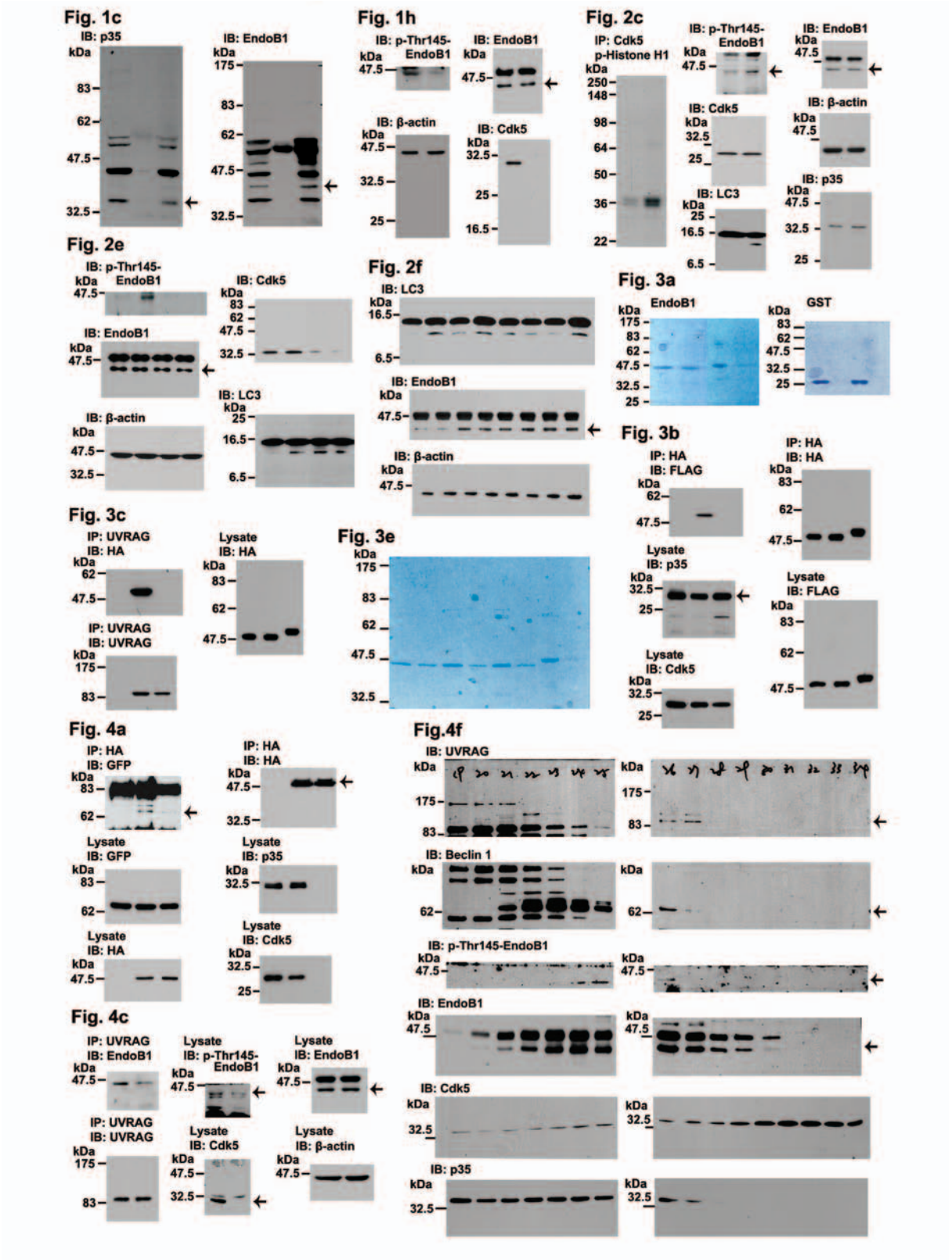

Figure S8 Full scan of immunoblots.

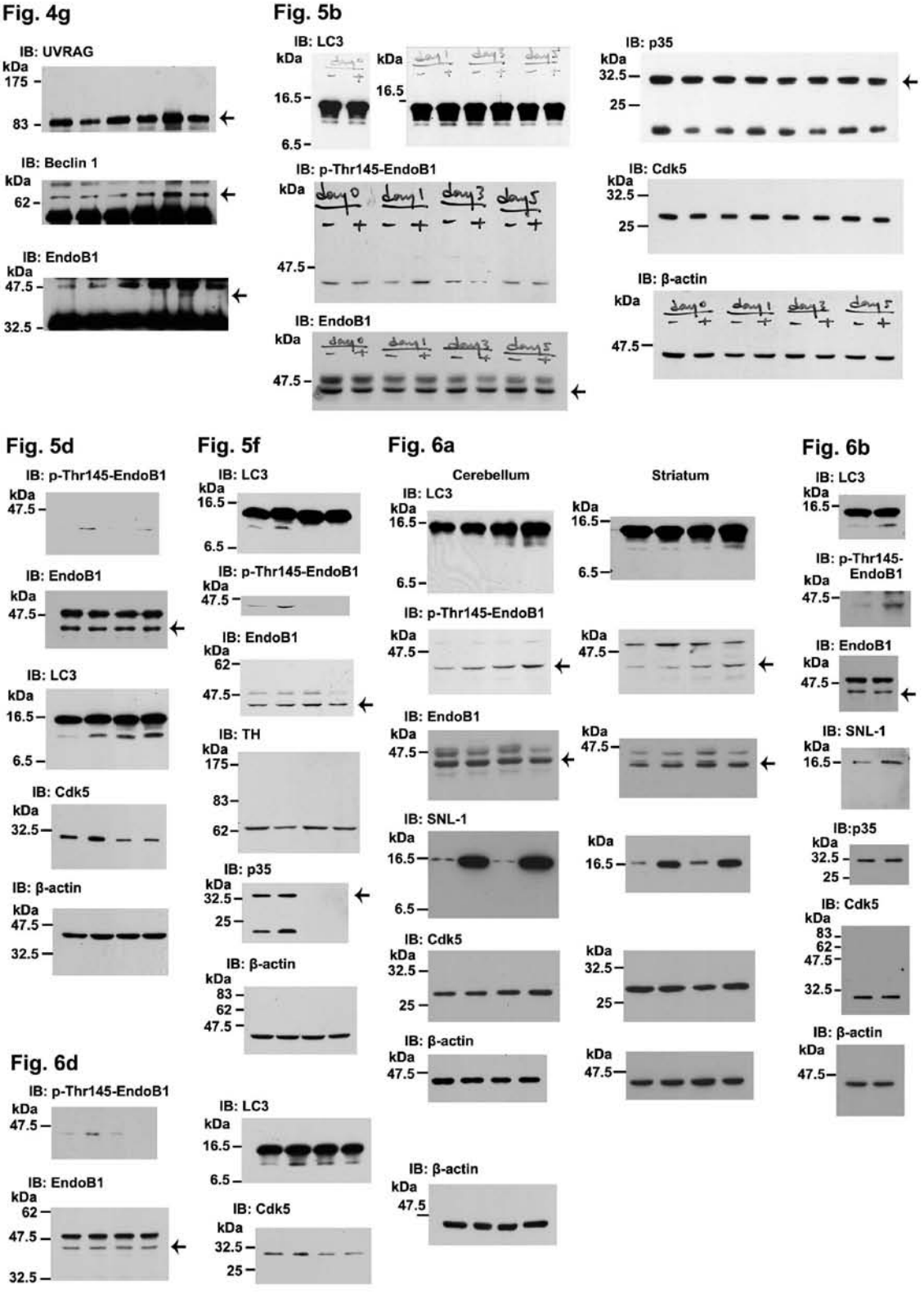

Figure S8 continued